iScience

Article

Single-cell transcriptome atlas of male mouse pituitary across postnatal life highlighting its stem cell landscape

Graphical abstract

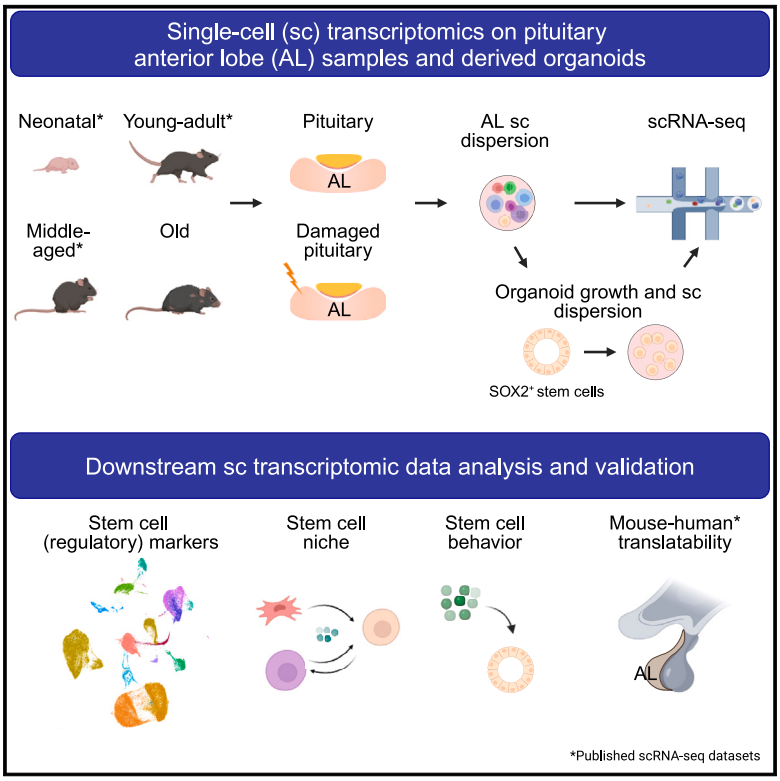

Highlights

- Single-cell transcriptome atlas of male mouse endocrine pituitary across key ages
- Pituitary stem cell identity and regulatory markers uncovered
- Stem cell niche interactions identified and functionally validated in organoids
- Increased inflammatory/immune phenotype in aging mouse and human pituitary

Authors

Silke De Vriendt, Emma Laporte, Berkehür Abaylı, Julie Hoekx, Florian Hermans, Diether Lambrechts, Hugo Vankelecom

Correspondence

hugo.vankelecom@kuleuven.be

In brief

Endocrine system physiology; Stem cells research; Transcriptomics

De Vriendt et al., 2025, iScience *28*, 111708
February 21, 2025
https://doi.org/10.1016/j.isci.2024.111708

CellPress

iScience

CellPress
OPEN ACCESS

Article

Single-cell transcriptome atlas of male mouse pituitary across postnatal life highlighting its stem cell landscape

Silke De Vriendt,[1,5] Emma Laporte,[1,5] Berkehür Abaylı,[1] Julie Hoekx,[1] Florian Hermans,[2] Diether Lambrechts,[3,4] and Hugo Vankelecom[1,6,*]

[1]Laboratory of Tissue Plasticity in Health and Disease, Cluster of Stem Cell and Developmental Biology, Department of Development and Regeneration, KU Leuven, 3000 Leuven, Belgium

[2]Department of Cardiology and Organ Systems (COS), Biomedical Research Institute (BIOMED), Faculty of Medicine and Life Sciences, Hasselt University, 3590 Diepenbeek, Belgium

[3]Laboratory for Translational Genetics, Department of Human Genetics, KU Leuven, 3000 Leuven, Belgium

[4]Center for Cancer Biology, Vlaams Instituut voor Biotechnologie (VIB), 3000 Leuven, Belgium

[5]These authors contributed equally

[6]Lead contact

*Correspondence: hugo.vankelecom@kuleuven.be

https://doi.org/10.1016/j.isci.2024.111708

SUMMARY

The pituitary represents the master gland governing the endocrine system. We constructed a single-cell (sc) transcriptomic atlas of male mouse endocrine pituitary by incorporating existing and new data, spanning important postnatal ages in both healthy and injured condition. We demonstrate strong applicability of this new atlas to unravel pituitary (patho)biology by focusing on its stem cells and investigating their complex identity (unveiling stem cell markers) and niche (pinpointing regulatory factors). Importantly, we functionally validated transcriptomic findings using pituitary stem cell organoids, revealing roles for Krüppel-like transcription factor 5 (KLF5), activator protein-1 (AP-1) complex and epidermal growth factor (EGF) pathways in pituitary stem cell regulation. Our investigation substantiated changes in stem cell dynamics during aging, reinforcing the inflammatory/immune nature in elderly pituitary and stem cells. Finally, we show translatability of mouse atlas-based findings to humans, particularly regarding aging-associated profile. This pituitary sc map is a valuable tool to unravel pituitary (patho)biology.

INTRODUCTION

The pituitary represents the core gland of the endocrine system, governing vital processes such as body growth, metabolism, sexual development, reproduction, stress, and immunity. To perform this key role, the gland houses various hormonal cell types. The major endocrine lobe (referred to as anterior lobe [AL]) comprises dedicated cell types that produce the different hormones encompassing growth hormone (GH, produced by somatotropes), prolactin (PRL; lactotropes), adrenocorticotropic hormone (ACTH; corticotropes), thyroid-stimulating hormone (TSH; thyrotropes), and luteinizing hormone (LH)/follicle-stimulating hormone (FSH; gonadotropes).[1–4] In addition, the organ contains non-hormonal cell types, including not only mesenchymal and endothelial cells but also stem cells. Despite their convincing assignment almost 20 years ago,[4] the stem cell population remains puzzling regarding molecular and functional nature.[5,6] The stemness transcription factor SOX2 is considered a general marker of pituitary stem cells, labeling cells that line the cleft (a remnant of the embryonically developing pituitary) as well as cell groups dispersed throughout the AL.[1,2,4–8] However, the cellular complexity of the stem cell compartment remains poorly charted.

Regarding stem-cell regulatory circuits, only fragmentary knowledge has been reported and a detailed picture is lacking.[9] Virtually nothing is known on the pituitary stem cell niche, or in other words which cell types interact with, and regulate, the stem cells, neither which regulatory signals rule in the niche. Recently, it has been shown that pituitary stem cells produce factors, among which wingless-type MMTV integration site family (WNT) pathway components, that, at least in the (mouse) maturing neonatal pituitary, activate proliferation of surrounding stem and endocrine (precursor) cells.[10,11] Thus, pituitary stem cells appear to act as auto-/paracrine signaling hub that regulates the behavior of own and neighboring cells. At present, this signaling role remains poorly depicted, as yet limited to the neonatal stage for WNT signaling.[10,11]

Regarding the typical stem-cell role, it has been shown that SOX2$^+$ stem cells are capable to self-renew and generate the different hormonal cell types in the gland. However, this contribution in tissue turnover appears low, especially in the adult homeostatic gland in which the stem cells show high dormancy.[1,2] By contrast, during the gland's maturation at neonatal age, the pituitary stem cells display an activated profile[10,12] and generate hormonal cells more prominently,[2,13] although the

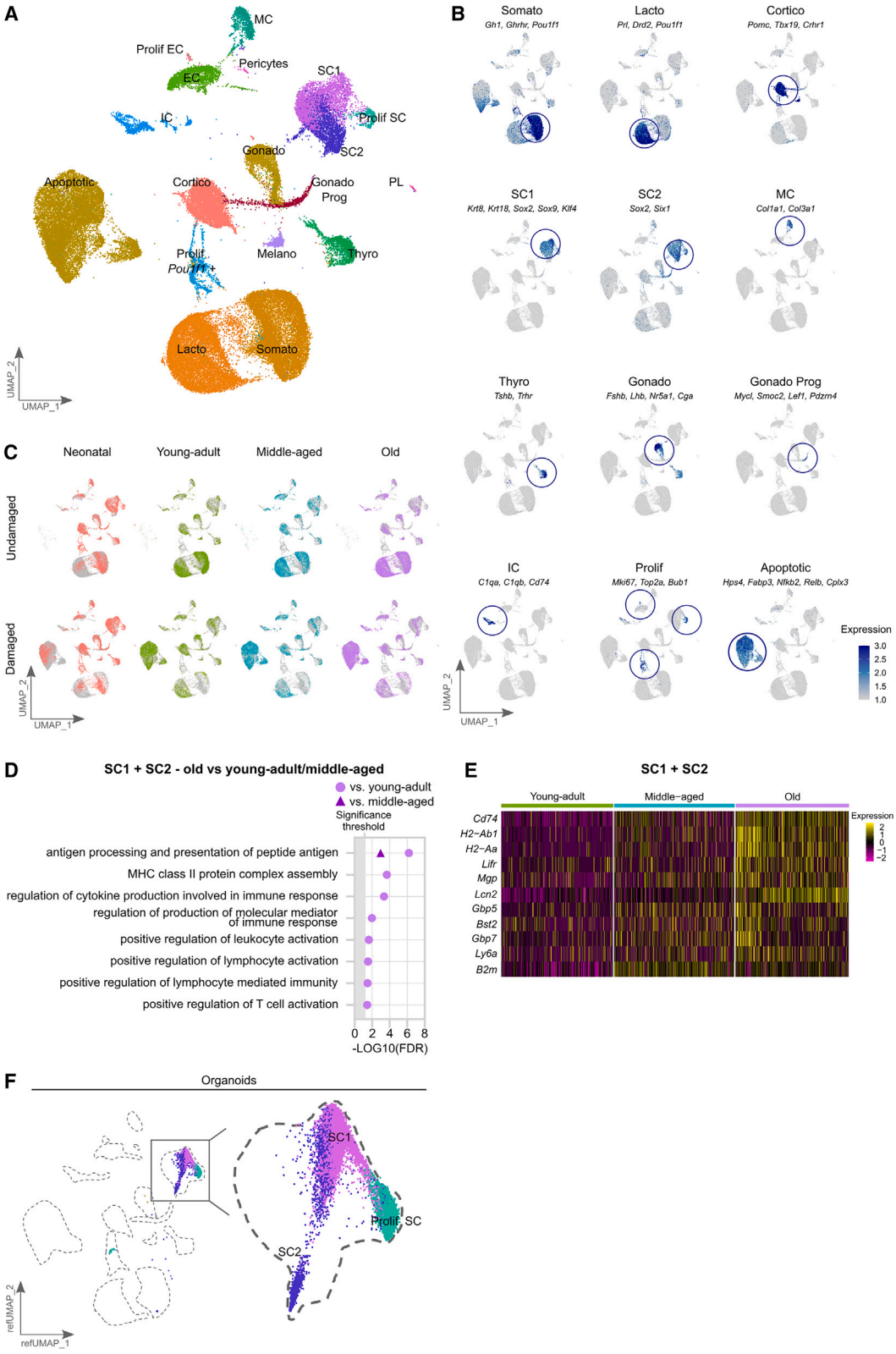

(legend on next page)

bulk of new endocrine cells still arises from already established lineage-committed precursor cells.[13] We and others have previously discovered that the pituitary stem cells become acutely activated when the gland is perturbed (e.g., after endocrine-cell ablation damage,[14–16] adrenalectomy,[1,17] and during tumorigenesis in the gland[2,18,19]), which may represent a first step in the ensuing tissue repair and regeneration process occurring after damage.

In addition, we found that the pituitary, as well as its stem cell compartment, suffers from an inflammatory phenotype at aging,[14] a process commonly referred to as "inflammaging",[20] which may explain the fading stem cell reaction and regenerative capacity as observed in the aging pituitary following locally inflicted damage.[14,16] This pituitary inflammaging process occurs in the mouse already at middle-age,[14,16] but it is not known what happens at still older ages.

Single-cell (sc) transcriptome technology provides a powerful tool to granularly depict the cellular landscape of organs. Although studies reporting sc transcriptomic data of mouse pituitary at certain ages,[10,14,17,21–26] or in genetically modified conditions,[27,28] have been published, a more overarching sc transcriptomic atlas across multiple postnatal time points is still missing. To fill this gap, we here built an extended sc map of the (male) mouse endocrine pituitary across several key postnatal ages (neonatal, young-adult and aging including middle-aged and elderly stages) in both healthy and challenged (injured) conditions. We integrated our previously published sc transcriptomic data (healthy unperturbed and injured/damaged neonatal,[10] young-adult and middle-age[14] AL; Table S1) with newly obtained datasets of elderly stages including healthy and injured pituitary (Table S1). Such extended sc atlases, achieved by combining published and newly acquired sc datasets, are being developed for manifold healthy and diseased tissues,[29–32] and provide valuable data compendia to unveil the (patho)biology of tissues in great cellular detail.

In our study, we show the strong potential and usefulness of the newly composed sc pituitary atlas by exploring the stem cell compartment's molecular identity and complexity, and the stem cell niche regulatory circuits. Importantly, we advanced several molecular findings into functional validation using our pituitary stem cell organoid model.[33,34] We have previously shown that pituitary organoids replicate the stem cells' phenotype and behavior,[10,14,18,34,35] thereby providing a powerful tool for pituitary stem cell inquiry including assessment of regulatory pathways and activation conduct. Compiling a mouse pituitary sc atlas across ages is also valuable to investigate mouse-human translatability through comparison against human pituitary sc/single-nucleus transcriptomic data at multiple ages,[36,37] which we also assessed here in a proof-of-principle approach. We also provide the sc map in an easily manageable loom format (using SCope[38]) allowing researchers to visualize the expression pattern of their genes of interest across the endocrine pituitary cell types and ages. Moreover, the newly composed pituitary sc map and datasets offer a rich resource for advanced bioinformatics to decode pituitary cell phenotypes, cellular complexities and regulatory networks across postnatal life. Eventually, a thorough understanding of the pituitary (stem) cells is not only essential to fully grasp the biology of this central endocrine organ, but also to gain insight into its burdening disorders, which may lead to new therapeutic prospects.

RESULTS

Single-cell map of the healthy and injured endocrine pituitary across postnatal life

Recently, we determined the sc transcriptomes of the major endocrine lobe of the pituitary (AL) from neonatal (postnatal day 7), young-adult (8–12 weeks) and middle-aged (12–15 months) mouse[10,14] of male sex except for neonatal age (with mixture of male and female pups) (Table S1). Here, we additionally performed scRNA-seq analysis of the AL from old male mouse (24–26 months), and integrated all datasets. In addition, the sc transcriptomes of injured old pituitary (i.e., following somatotrope-cell ablation damage using the $Gh^{Cre/+};R26^{iDTR/+}$ transgenic mouse model[15]) was determined, as done before for the younger ages.[10,14] These damaged pituitary sc datasets across all targeted ages were added to the unperturbed (undamaged) pituitary sc datasets (See Graphical Abstract; Table S1).

Rigorous quality control to filter out low-quality cells, doublets and ambient RNA yielded 67,374 qualified cells (Figure S1A; Table S1). Unsupervised clustering pinpointed 18 cell groups (Figure 1A) which were annotated using canonical markers[10,14,21] and depicted by expression of gene marker signatures (referred to as "gene modules"; Figures 1B and S1B). All pituitary endocrine cell types as well as non-hormonal cells including endothelial, immune, and stem cells were distinguished (Figures 1A, 1B, and S1B). The stem cell population was found to subcluster in 3 groups as previously reported,[10,14] designated as SC1, SC2, and proliferating (prolif) SC, the latter predominantly restricted to the neonatal pituitary (Figures 1A–1C). A small number of cells from the intermediate lobe (melanotropes) and the posterior lobe were also detected (Figure S1B), likely due to limited residual

Figure 1. Single-cell map of the healthy and injured endocrine pituitary across postnatal life

(A) UMAP plot of AL from neonatal, young-adult, middle-aged and old mouse in healthy and injured conditions ($n = 2$ biological replicates for each experimental condition). Cortico, corticotropes; EC, endothelial cells; Gonado (Prog), gonadotrope(s) (progenitors); IC, immune cells; Lacto, lactotropes; MC, mesenchymal cells; Melano; melanotropes; PL, posterior lobe cells; Prolif, proliferating; SC1 and SC2, stem cell cluster 1 and 2; Somato, somatotropes; Thyro, thyrotropes.

(B) Cell clusters annotated with top marker genes visualized with module scores ("gene modules"). Average expression is indicated by color intensity (see scale).

(C) UMAP plots visualizing AL sample distribution.

(D) Upregulated differentially expressed gene (DEG)-associated gene ontology (GO) biological processes and terms associated with immune-related processes in SC1 + SC2 of (undamaged) old versus young-adult or middle-aged AL. FDR, false discovery rate; MHC, major histocompatibility complex.

(E) Heatmap displaying relative gene expression (see color scale) related to GO terms involving MHC-II complex assembly and inflammatory/cytokine response in SC1 + SC2 of (undamaged) young-adult, middle-aged and old AL.

(F) UMAP plot showing the pituitary organoid cells projected onto the primary pituitary sc map. refUMAP, reference Uniform Manifold Approximation and Projection. See also Figure S1, Tables S1, and S2.

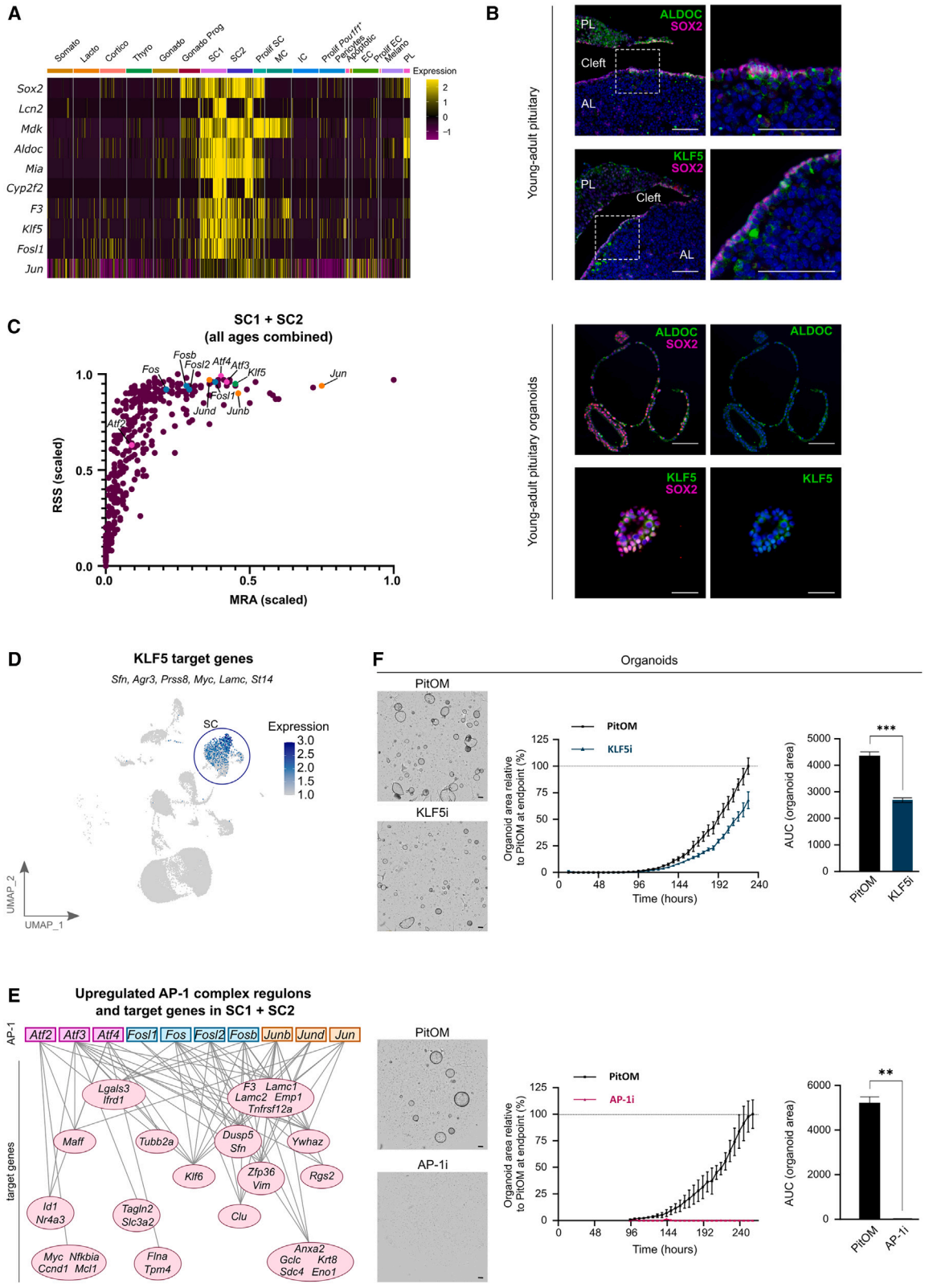

(legend on next page)

tissue still connected to the AL at dissection. Cells from each dataset (i.e., from the different ages and conditions) seamlessly integrated within their corresponding clusters, with a large cell cluster of apoptotic cells surfacing in the damaged pituitary condition as expected (Figures 1A–1C).

We previously discovered that the (undamaged) pituitary displays an inflammatory phenotype in middle-aged mice, reminiscent of the general process of gradually increasing tissue inflammation at aging (inflammaging).[14,20] In particular, we detected a prominent inflammatory nature in the stem cells at middle age when compared to young-adult stage.[14] To assess this process at still older age, we applied gene ontology (GO) analysis to differentially expressed genes (DEGs) between old and young-adult/middle-aged stem cells (SC1 + SC2). This GO interrogation revealed that the old pituitary's stem cell population exhibits enrichment of immune system/cell-related terms (Figure 1D; Tables S2A and S2B), along with the upregulation of genes involved in assembly of major histocompatibility complex (MHC) class II protein, and antigen processing and presentation of peptide antigen (e.g., histocompatibility 2 class II antigen gamma [*Cd74*], antigen A beta 1 [*H2-Ab1*], H2 A alpha [*H2-Aa*], beta-2 microglobulin [*B2m*]) (Figure 1E; Tables S2A and S2B). A similar immune system-related enrichment with aging has been observed in mouse intestinal stem cells,[39] and immune cells are known to play an important role in inflammaging.[40,41] Accordingly, we detected an increasing number of immune cells at aging in the pituitary (Figure S1C). Subclustering of the immune cell population revealed a predominant abundance of monocytes while other immune cell types (i.e., neutrophils and natural killer [NK], B and T cells) were scarcer (Figures S1C and S1D). Also, inflammatory/cytokine response genes (such as leukemia inhibitory factor receptor (*Lifr*), matrix gla protein (*Mgp*), lipocalin 2 (*Lcn2*), guanylate binding protein 5/7 (*Gbp5/7*), bone marrow stromal cell antigen 2 (*Bst2*) and lymphocyte antigen 6 family member A (*Ly6a*) were found upregulated in old pituitary stem cells (Figure 1E; Table S2A). Together, these findings further underpin the rising inflammatory state of pituitary stem cells at aging.

Previously, we established a pituitary stem cell organoid model that closely recapitulates the molecular and functional phenotype of the pituitary stem cells,[34] such as their activated nature during neonatal maturation,[10] local damage[14] and tumorigenesis in the gland.[18] Hence, these pituitary (SOX2$^+$) stem cell-derived organoids provide a powerful *ex vivo* tool for molecular, functional and regulatory inquiry of the pituitary stem cell population.[33] Here, we performed scRNA-seq analysis of organoids derived from the (undamaged) pituitary (AL) across the targeted ages (See Graphical Abstract). Projection of the organoid sc transcriptomes onto the pituitary scRNA-seq atlas showed clear alignment of the organoid cells with the pituitary stem cells, covering SC1, SC2, and prolif SC (Figures 1F and S1E). Of note, prolif SC make up a larger proportion due to the specific stem cell-stimulating conditions used, and needed, to culture and grow the organoids.

Together, our newly built pituitary sc atlas, depicting the distinct cell populations across multiple postnatal ages, reinforces the immune/inflammatory phenotype in pituitary stem cells at aging, thus offering an interesting tool to explore inflammaging (and other processes) occurring at aging. Furthermore, pituitary organoid cells highly align with primary stem cell populations, thereby leveraging the organoid model as powerful platform to deeply investigate molecular and functional aspects of pituitary stem cells.

Applying the pituitary single-cell atlas to unveil pituitary stem cell markers

Although discovered almost 20 years ago,[4] pituitary stem cells' cellular composition, regulatory circuit and functional role are still poorly charted and understood.[5,6,9] Our established pituitary sc atlas presents a valuable tool to fill these gaps.

Differential gene expression analysis between the pituitary's stem cell clusters and the other cell types revealed 392 upregulated DEGs common to all ages (Figure S2A; Table S3A), encompassing some previously reported[17,21] but still poorly documented stem cell markers (such as midkine [*Mdk*], aldolase c [*Aldoc*] and Krüppel-like transcription factor 5 [*Klf5*]) (Figure 2A; Table S3A). While *Sox2*, *Lcn2*, *Mdk*, *Aldoc*, melanoma inhibitory activity (*Mia*) and cytochrome P450 family 2 subfamily f polypeptide 2 (*Cyp2f2*) are commonly expressed in both SC1 and SC2, coagulation factor III (*F3*), *Klf5* and Fos-like 1 (*Fosl1*) appear more prominent in SC1, and *Jun* (as well as *Fos*) in SC2 (Figures 2A, S2B, and Table S4). The expression pattern

Figure 2. Pituitary stem cell markers

(A) Heatmap displaying scaled expression (see color scale) in the pituitary stem cell clusters compared to all other pituitary cell types (of undamaged pituitary, all ages combined).

(B) Immunofluorescence staining of SOX2 (magenta) together with ALDOC or KLF5 (green) in (undamaged) young-adult pituitary and derived organoids. Nuclei are labeled with Hoechst33342 (blue) (scale bar, 100 μm). Boxed area in young-adult pituitary is magnified in right panels. Separate ALDOC and KLF5 signals are shown in organoids in right panels. AL, anterior lobe; PL; posterior lobe.

(C) Scatterplot of scaled regulon specificity score (RSS) and scaled mean regulon activity (MRA) in SC1 + SC2 (of undamaged pituitary, all ages combined) with each dot indicating an individual regulon. Specific regulons are indicated by color and annotated genes shown, including AP-1 complex subunits (*Atf* family, magenta; *Fos* family, cyan; *Jun* family, orange) and *Klf5* (green).

(D) UMAP displaying expression of *Klf5* target genes, visualized by module score (see color scale).

(E) Network visualization of significantly upregulated regulons (rectangles) involved in AP-1 complex and their target genes (ovals) in SC1 + SC2 versus the other cell types (*Atf* family, magenta; *Fos* family, cyan; *Jun* family, orange).

(F) Organoid development and growth from young-adult AL in the absence (PitOM) or presence of KLF5 inhibitor (KLF5i) (*top*). Organoid development and growth from young-adult AL in the absence (PitOM) or presence of AP-1 inhibitor (AP-1i) (*bottom*). Representative brightfield pictures of organoid cultures on day 10–11 (scale bar, 200 μm; *left*) and quantification of organoid area (relative to PitOM at endpoint) over time in culture are shown. Bar plots represent absolute area under the curve (AUC) calculated from organoid area ($n = 3$ biological replicates per treatment; *right*). Mean ± standard error of the mean (SEM) is depicted. $^{**}p \leq 0.01$; $^{***}p \leq 0.001$; unpaired, two-tailed Student's t test. See also Figure S2, Tables S3, S4, and S5.

of the top 10 DEGs in the stem cell subclusters is supportive of a molecular relationship (or continuum of stem cell states) between SC1, SC2, and prolif SC (Figure S2B; Table S4). In addition to the common DEGs across the ages, the stem cells also display age-specific expression characteristics (Figure S2A; Table S3A). For example, *Lcn2* and *Cyp2f2* are upregulated in stem cells of young-adult, middle-aged, and old mice as compared to the remaining cell types, but not in neonatal pituitary (Figure S2A). Stem cells of old pituitary show expression of histocompatibility 2–Q region locus (*H2-Q4/6*) and NCK adaptor protein 2 (*Nck2*) (Figure S2A; Table S3A), both associated with the GO term ''positive regulation of T cell activation'' which is enriched in the old pituitary stem cells (Figure 1D; Table S2B), and in line with our finding of risen immune cell proportion in the elderly gland (Figure S1C). Neonatal stem cells show increased expression of genes involved in ''regulation of stem cell maintenance'' and ''stem cell differentiation'' including genes of the important stem cell- and embryogenesis-regulating WNT and sonic hedgehog (SHH) pathways (e.g., frizzled class receptor 2 [*Fzd2*] and smoothened [*Smo*], respectively) and other regulatory growth factors (e.g., Erb-B2 receptor tyrosine kinase 4 [*Erbb4*], fibroblast growth factor receptor 2 [*Fgfr2*]) (Figure S2A). Expression of Hippo pathway-related genes, such as TEA domain transcription factor 2 (*Tead2*) and downstream target genes,[42] is also enriched in the stem cell compartment of neonatal pituitary compared to later ages (Figures S2A and S2C).

To validate sc transcriptome-based observations, we assessed protein expression in both primary pituitary tissue and organoids. The glycolytic enzyme ALDOC, identified as a marker of quiescent neural stem cells[43] and formerly reported in (rat) pituitary folliculostellate (FS) cells[44] (which are considered to overlap, at least partially, with the pituitary stem cell population[5,9,45]), was *in situ* observed in the ($SOX2^+$) stem cells (lining the cleft; Figure 2B), in accordance with its prominent expression in the stem cell cluster in the sc transcriptome data (Figure 2A). KLF5, previously shown to regulate stemness of (mouse) intestinal[46] and embryonic stem cells,[47] was also detected in the pituitary's stem cells (Figure 2B), thereby also validating the scRNA-seq-based conclusions (Figure 2A). Both proteins were also uncovered in the pituitary-derived stem cell organoids (Figure 2B). The organoids' stem cell subclusters largely recapitulate the expression pattern of the markers as occurring in the *in vivo* stem cells (e.g., *Lcn2* and *Cyp2f2* commonly expressed in both SC1 and SC2, while *Klf5* and *Fosl1* more prominently expressed in SC1; Figure S2D). *Aldoc*, *Jun*, and *Fos* expression in the organoids appears more prominent in SC1 than found *in vivo.* Expression of these *in vivo* stem cell markers was validated in the organoids by reverse transcription quantitative PCR (RT-qPCR) and found across all ages (Figure S2D).

Gene-regulatory networks (termed ''regulons''), as orchestrated by key transcription factors that determine cell identity and biology, were assessed using pySCENIC.[48] Among others, pronounced regulon activity of *Klf5*, and of *Fos*/*Fosl1*/*Jun*/activating transcription factor (*Atf*) members which are together part of the activator protein-1 (AP-1) transcription factor complex, was detected in the stem cell population (as assessed in SC1 + SC2 which are present at all ages, thus without the mainly neonatal prolif SC) (Figure 2C; Table S5), aligning with the expression findings of these factors (Figure 2A). Multiple downstream target genes of *Klf5* (e.g., stratifin [*Sfn*], anterior gradient 3 [*Agr3*], *Myc*) were significantly upregulated in stem cells compared to the other cell types (Figure 2D). Also, many of the downstream target genes of the different regulons of the AP-1 complex subunits were significantly upregulated in stem cells (Figure 2E). The functional importance of the prominently active *Klf5* and *Fos*/*Fosl1*/*Jun*/*Atf* regulons was investigated using our pituitary stem cell-assessing organoid tool. Adding a small-molecule KLF5 inhibitor (KLF5i) reduced organoid growth capacity, while inhibition of AP-1 activity (AP-1i) abolished organoid development and growth (Figure 2F). Hence, both core transcriptional regulators are considered important in pituitary stem cell regulation/growth.

Previously, we have shown that the young-adult pituitary stem cells are acutely activated upon locally inflicted damage (by somatotrope-cell ablation) with increased proliferative activity and expansion,[14,15] whereas no and lower responses were observed at neonatal and middle age, respectively.[10,14,16] Our sc atlas confirmed these findings of presence or absence of an overt stem-cell expansive reaction (proportion; Figure S2E). The highest number of DEGs in the stem cell population of damaged versus undamaged pituitary was found in the young-adult mouse (Figure S2F; Table S6A), in line with the stem cell reaction being most prominent at this age.[14–16] Using our new atlas, we could confirm the upregulated expression of paired related homeobox 2 (*Prrx2*) (Figures S2F and S2G) in the stem cell population of young-adult pituitary after local damage as found in previous work,[34] hypothesized to be involved in the stem cell activation reaction. The middle-aged and old pituitary showed *Prrx2* upregulation as well, although to a lower extent (Figure S2G), which is in line with the lower stem cell activation reaction at these ages.[14,16] Multiple genes related to inflammation (e.g., interleukin 13 receptor subunit alpha 1 (*Il13ra1*), Z-DNA binding protein 1 (*Zbp1*), tachykinin precursor 1 (*Tac1*), proteasome 20S subunit beta 8 (*Psmb8*), *H2-Q4*) were found significantly upregulated upon local damage in the young-adult pituitary stem cells (Figures S2F and S2G; Table S6A). This inflammatory stem-cell response to damage supports our previous observations which have led to the identification of IL-6 as pituitary stem cell-activating factor.[14] Importantly, these inflammatory genes are already considerably expressed in the stem cell compartment at older ages in the undamaged gland (as part of inflammaging) (Figures S2A, S2F, and S2G) and therefore not capable anymore of substantial upregulation in response to injury, a condition which may underlie the faded activation reaction of the stem cells at aging (as shown before for IL-6[14]). Of note, some DEGs in the neonatal damaged versus undamaged pituitary are sex-related (i.e., X inactive specific transcript (*Xist*), XIST antisense RNA (*Tsix*) and DEAD-box helicase 3 Y-linked (*Ddx3y*); Table S6A), accounted for by the presence of a female pituitary sample (i.e., DMG1) among the neonatal samples (as revealed using the sc expression data; Figure S2H). Nevertheless, removing this female sample from the analysis did not overtly change the DEGs or conclusions (Table S6B), in particular that neonatal pituitary stem cells do almost not react to damage, showing only a limited number of DEGs compared to

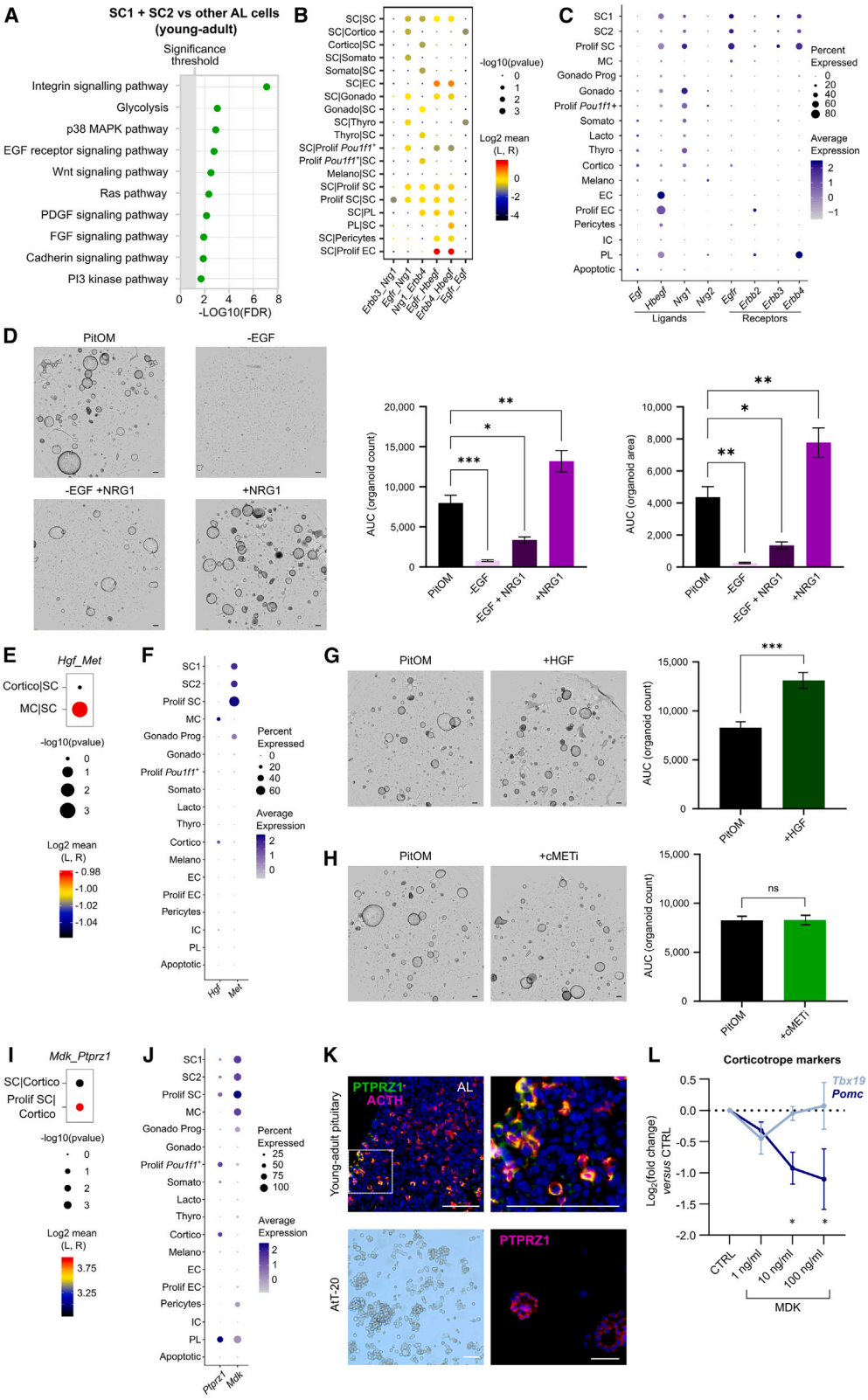

(legend on next page)

undamaged neonatal pituitary, likely due to the already high stem cell activation state at this early age.[10]

Taken together, the stem cell transcriptome as provided in the newly built pituitary sc atlas, both from primary tissue and organoids, is highly valuable to delve deeper into the stem cells' phenotypical, functional and regulatory complexity. In addition, the organoid model enables to functionally validate molecular findings extracted from the pituitary stem cell transcriptomics.

Applying the pituitary single-cell atlas to unveil cellular crosstalk and regulatory circuits in the pituitary stem cell niche

The pituitary sc transcriptome atlas can provide insight into the pituitary stem cell niche, more particularly into the stem cell-regulatory factors in the niche and the cell types that crosstalk with the stem cells to regulate their biology. In addition, the sc atlas can predict signaling from stem cells as signaling hub toward other cell types (as well as between stem cells themselves).

GO analysis of DEGs between the stem cell population and all other pituitary cell types (as applied to the undamaged young-adult AL) confirmed previously described enrichment of the WNT signaling pathway in stem cells (Figure 3A; Table S3B).[10,11,14] The WNT pathway may underlie auto- and paracrine regulatory activity executed by the stem cells (as recently demonstrated in neonatal pituitary[10,11]). The stem cell-originating regulatory circuit may further encompass epidermal growth factor (EGF) receptor (EGFR), FGF, phosphoinositide 3 (PI3) kinase and platelet-derived growth factor (PDGF) signaling pathways, all enriched in the stem cell compartment (Figure 3A). In addition, biological processes related to cell adhesion and communication with the extracellular matrix such as integrin and cadherin signaling pathways are enriched in pituitary stem cells (Figures 3A and S3A). Analogous DEG-based biological term enrichments were found in the stem cell population at other ages (Figure S3A).

To uncover putative interactions between the endocrine pituitary's stem cells and other cell types, we performed CellPhoneDB analysis[49] which integrates cell type-specific ligand/receptor expression and calculates ligand/receptor pair scores, thereby predicting cell-cell crosstalk patterns. The interrogation revealed manifold projected interactions between all pituitary cell types, with (proliferating) stem cells also showing high numbers (Figure S3B; Table S7). Our analysis validated previously reported pathways found key in pituitary stem cell biology (including NOTCH, WNT, FGF, and ephrin (EPH)-related pathways)[9] (Figure S3C), as well as provided new insights into the specific ligand-receptor pairs associated with these pathways, together with the identity of the specific cell type with which the stem cells interact.

CellPhoneDB analysis uncharted multiple EGF pathway ligand-receptor interactions among the stem cells themselves, and between stem cells and other cell types (Figure 3B; Table S7). In addition, the EGFR pathway is enriched within the stem cell compartment (Figure 3A; Table S3B). Therefore, we investigated this candidate regulatory circuit as proof-of-concept to utilize the atlas for unraveling stem-cell niche regulatory networks. Transcriptome expression analysis of the EGF pathway family

Figure 3. Cellular crosstalk and regulatory circuits in the pituitary stem cell niche

(A) Upregulated DEG-associated GO biological processes and terms in SC1 + SC2 versus all other AL cells (undamaged young-adult pituitary).

(B) Dotplot displaying predicted ligand-receptor pairs of the EGF family involved in crosstalk between the stem cells (SC1 + SC2, here referred to as SC) and other cell clusters, as inferred by CellPhoneDB (undamaged pituitary, all ages combined). Dot size represents –log10 of *p* values and color intensity (see scale) indicates mean of average expression of ligand and receptor.

(C) Dotplot displaying average expression (color intensity, see scale) of EGF family ligands and receptors and percentage of cells (dot size) within the AL cell clusters expressing the specified gene (undamaged pituitary, all ages combined).

(D) Organoid development and growth from young-adult AL in pituitary organoid medium (PitOM; containing EGF), in PitOM without EGF (-EGF), in PitOM without EGF supplemented with NRG1 (-EGF +NRG1) or in PitOM (containing EGF) with NRG1 (+NRG1). Representative brightfield pictures of organoid cultures (day 10; scale bar, 200 μm; *left*) are shown. Bar plots represent the calculated AUC of organoid number (count) and total organoid area (biological replicates per treatment, $n = 3$; *right*). Mean ± SEM is depicted. $^{*}p \leq 0.05$, $^{**}p \leq 0.01$; $^{***}p \leq 0.001$; one-way ANOVA with Dunnett's multiple comparisons test.

(E) Dotplot displaying predicted *Hgf-Met* ligand–receptor interaction between stem cells (SC1 + SC2, here referred to as SC) and corticotropes (Cortico) or mesenchymal cells (MC), as inferred by CellPhoneDB. Dot size represents –log10 of *p* values and color intensity (see scale) indicates mean of average expression of *Hgf* and *Met*.

(F) Dotplot displaying average expression (color intensity, see scale) of *Hgf* and *Met* and percentage of cells (dot size) within the AL cell clusters expressing *Hgf* and *Met* (undamaged pituitary, all ages combined).

(G) Organoid number growing from young-adult AL in absence (PitOM) and presence of HGF (+HGF). Representative brightfield pictures of organoid cultures (day 10; scale bar, 200 μm; *left*) are shown. Bar plot represents the calculated AUC of organoid number (biological replicates per treatment, $n = 6$; *right*). Mean ± SEM is depicted. $^{***}p \leq 0.001$; unpaired, two-tailed Student's t test.

(H) Organoid number growing from young-adult AL in absence (PitOM) and presence of cMET inhibitor (+cMETi). Representative brightfield pictures of organoid cultures (day 10; scale bar, 200 μm; *left*) are shown. Bar plot represents the calculated AUC of organoid number (biological replicates per treatment, $n = 6$; *right*). Mean ± SEM is depicted. ns, non-significant; unpaired, two-tailed Student's t test.

(I) Dotplot displaying predicted *Mdk-Ptprz1* interaction between (proliferating) stem cells (SC1 + SC2, here referred to as SC, and Prolif SC) and corticotropes (Cortico), as revealed by CellPhoneDB. Dot size represents –log10 of *p* values and color intensity (see scale) indicates mean of average expression of *Mdk* and *Ptprz1*.

(J) Dotplot displaying average expression (color intensity, see scale) of *Mdk* and *Ptprz1* and percentage of cells (dot size) within the AL cell clusters expressing *Mdk* and *Ptprz1* (undamaged pituitary, all ages combined).

(K) Immunofluorescence staining of PTPRZ1 (green; *top*) and ACTH (magenta; *top*) in young-adult pituitary. Boxed area is magnified. Representative brightfield image of AtT-20 live cell culture (*bottom left*) and immunofluorescence staining of PTPRZ1 in fixed AtT-20 cells (magenta; bottom *right*). Nuclei are labeled with Hoechst33342 (blue) (scale bar, 100 μm). AL, anterior lobe.

(L) Gene expression level of corticotrope (precursor) markers (*Tbx19*, *Pomc)* in AtT-20 cells as determined by RT-qPCR in the absence (control (CTRL)) or presence of MDK at increasing concentrations ($n = 3$ biological replicates per treatment). Mean ± SEM is depicted. $^{*}p \leq 0.05$; two-way ANOVA with Šídák's multiple comparisons test. See also Figure S3, Tables S3, and S7.

members revealed prominent expression of the receptors *Egfr* and *Erbb3/4* in the stem cell population (Figure 3C). Among the ligands, *Egf* is expressed in several endocrine cell types (although at low abundance), whereas heparin-binding EGF-like growth factor (*Hbegf*) and neuregulin 1 (*Nrg1*) are more prominently expressed in different cell types including endocrine and endothelial cells as well as stem cells (Figure 3C). Functional interrogation of the EGF circuit was performed using the pituitary organoid model. Organoids showed a comparable expression pattern regarding ligands (e.g., very low expression of *Egf* and *Nrg2*, and highest expression of *Hbegf* and *Nrg1* in SC1 and prolif SC when compared to SC2) and receptors (e.g., prominent expression of *Egfr* and *Erbb3*, both lowest in the SC2) (Figure S3D). On the other hand, expression of *Erbb4* became much lower in organoid culture (Figure S3D). Previously, we have found that outgrowth of pituitary stem cells into organoids, and their further expansion, requires the presence of EGF.[34] In line, removal of EGF ("-EGF") from the defined pituitary organoid medium (PitOM) (Figures 3D and S3E), or inhibition of the PitOM-included EGF (with EGFR inhibitor ("+EGFRi"); Figure S3F), virtually abolished organoid development. We have previously also shown that HBEGF could substitute for EGF in organoid development and growth, although not fully,[34] which may be (at least partly) due to the only low expression of *Erbb4* in the organoids (Figure S3D) as one of the mediating receptors of HBEGF activity. Here, we found that NRG1 can also only partially rescue organoid development in the absence of EGF ("-EGF + NRG1") (which may also (partly) be due to the very low *Erbb4* expression, being one of the transducing receptors of NRG1 activity), while adding NRG1 to PitOM (the latter containing EGF; "+NRG1") elevated organoid growth beyond the action of EGF alone (i.e., in PitOM) (Figures 3D and S3E), likely due to cumulative activation of the different EGF family receptors that are present (acting as dimers). Together, our results provide evidence that the EGF family pathway represents one of the regulatory circuits within the pituitary stem cell niche.

Given the enrichment of the hepatocyte growth factor (HGF) downstream PI3K pathway in the stem cells (Figure 3A), as well as the recently described stimulatory effect of HGF on pituitary stem cells (in the context of the impact of adrenalectomy[17]), we looked into the HGF-cMET interaction (i.e., cMET receptor and its selective ligand HGF[50]) using CellPhoneDB (Figure 3E) and found a predicted crosstalk between corticotropes or mesenchymal cells (MC), both expressing *Hgf*, and stem cells, in which *Met* is indeed most prominently expressed when compared to the other cell types (Figures 3E and 3F). We functionally validated the relevance of HGF-cMET signaling for pituitary stem cells using organoids, found to recapitulate expression of *Met* (Figure S3G). Adding HGF ("+HGF") resulted in increased organoid outgrowth (Figures 3G and S3H). Supplementing a cMET inhibitor ("+cMETi") to the standard condition (i.e., PitOM, which does not contain HGF) did not affect organoid development and growth (Figures 3H and S3I), indicating that cMET is not constitutively active in the stem cells and needs exogenous (non-stem cell-originating) HGF, which is in line with the virtual absence of *Hgf* expression in the stem cells and derived organoid cultures (Figures 3F and S3G). Together, these findings provide evidence that cMET activation is a regulator of pituitary stem cell biology with HGF as upstream factor secreted by other cells, in particular corticotropes and MC, cell populations that thus appear to represent important regulatory actors in the pituitary stem cell niche. Interestingly, we also identified a highly predicted communication from somatotropes (and their proliferating *Pou1f1*$^+$ progenitor cells) toward stem cells through *Gh1*-GH receptor (*Ghr*) interaction (Figure S3C), suggesting the involvement of somatotropes in the regulation of stem cells by their specific hormone.

As mentioned, the stem cell population was recently advanced to act as signaling hub, not only within the stem cell compartment itself (e.g., through WNT signaling; [10] Figure 3A), but also toward other cells, as particularly shown for committed (POUF1F1$^+$/PIT1$^+$) progenitor cells also through WNT.[11] Here, CellPhoneDB analysis projected a candidate communication from (proliferating) stem cells to corticotropes through MDK, one of the stem cell markers (Figure 2A), and its corresponding receptor protein tyrosine phosphatase receptor type Z1 (PTPRZ1) (Figure 3I). *Mdk* is indeed prominently expressed in the stem cell population (and MC) as compared to the other cell types, while *Ptprz1* is highly expressed in corticotropes (among some other cell types; Figure 3J), further validated by immunostaining showing its presence in ACTH$^+$ cells in the pituitary and in the mouse corticotrope AtT-20 cell line (Figure 3K). Adding MDK to AtT-20 cells did not affect cell number nor expression of proliferation markers (Figure S3J). However, MDK dose-dependently reduced gene expression of the mature corticotrope marker proopiomelanocortin (*Pomc*), the ACTH precursor molecule, without significantly affecting the corticotrope progenitor/fate marker T-box transcription factor 19 (*Tbx19*) (Figure 3L). Thus, stem cells may signal to corticotropes through MDK to retain the cells in, or reverse them to, a progenitor state.

Taken together, our newly built pituitary sc atlas enables to decode interactions between pituitary stem cells and other local cell types, thereby portraying the stem cell niche, and will in the same manner also empower similar analyses between non-stem cell types among each other.

Translating mouse pituitary atlas findings to human pituitary

To further show the applicability of this mouse pituitary sc atlas, we addressed the question whether mouse pituitary-based findings are translatable to human pituitary in a few proof-of-principle approaches by using available human pituitary sc/single-nucleus transcriptome datasets.[36,37] Before, we already showed that mouse neonatal and human fetal pituitary sc data[37] can be integrated, thereby revealing similar expression patterns of WNT-associated genes.[10] Here, we further tested mouse-human translation by first analyzing the stem cell markers of mouse pituitary (Figure 2A) in the human fetal[37] and postnatal (pediatric, adult, and old[36]) datasets. Overall, despite the absence of stem cell compartment division in SC1 and SC2 in the human datasets, *KLF5* and *F3* show comparable enrichment in human pituitary stem cells (Figures 4A and 4B), but also expression in other cell types such as MC which is also found in mouse (Figure 2A). The general pituitary stem cell marker *SOX2* appears more prominently enriched in the stem cell compartment of human fetal than postnatal pituitary (Figures 4A and 4B). The other mouse pituitary stem cell markers show less correspondence

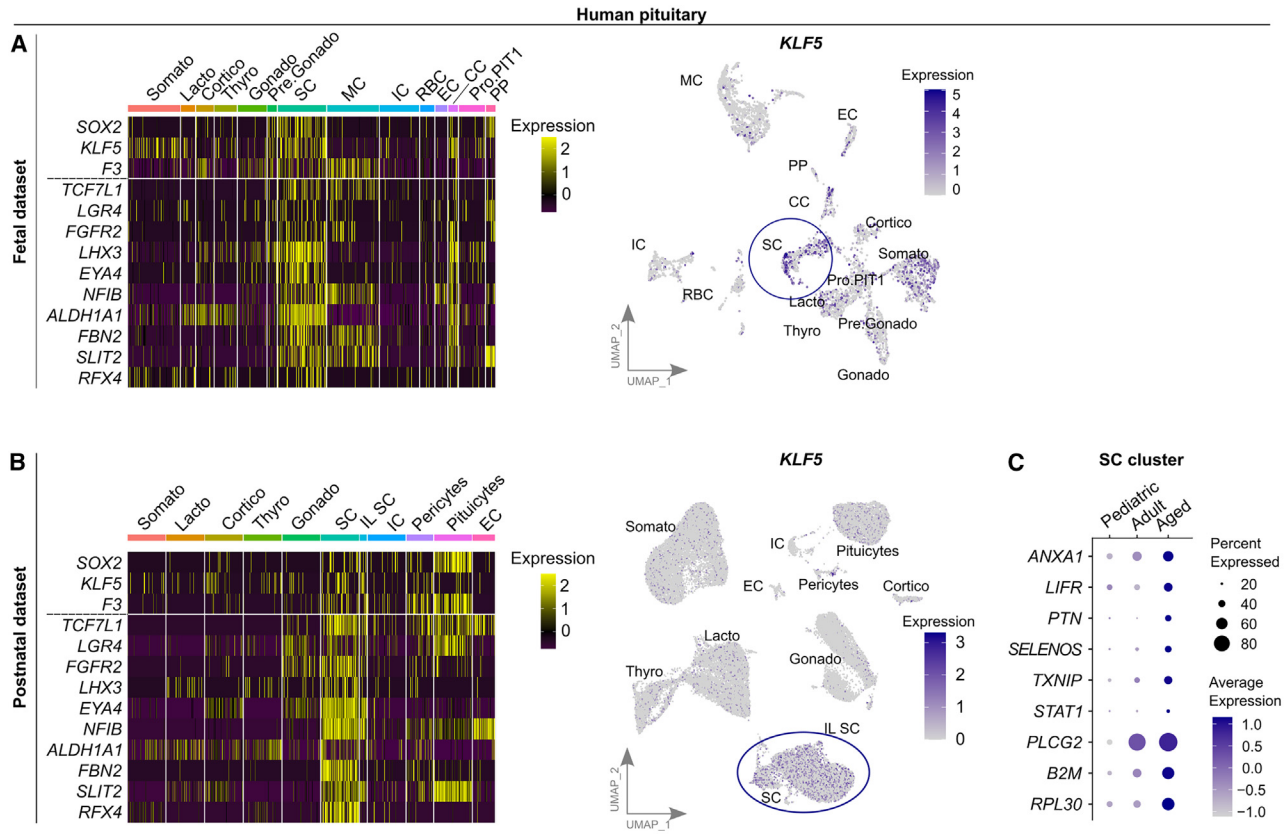

Figure 4. Translating mouse pituitary atlas findings to human pituitary

(A) Heatmap displaying scaled expression (see color scale) of stem cell markers (from mouse pituitary above the line, common to mouse and human pituitary below the line) in cell clusters of human fetal pituitary (dataset from[37]) (*left*). Featureplot of human fetal pituitary visualizing expression of *KLF5* (see color scale). CC, cycling cells; Cortico, corticotropes; EC, endothelial cells; IC, immune cells; Lacto, lactotropes; MC, mesenchymal cells; (Pre.) Gonado, (precursor of) gonadotropes; PP, posterior pituitary cells; Pro. PIT1, progenitors of the PIT-1 lineage; RBC, red blood cells; SC, stem cells (encircled); Somato, somatotropes; Thyro, thyrotropes.

(B) Heatmap displaying scaled expression (see color scale) of stem cell markers in cell clusters of human postnatal pituitary (dataset from[36]) (*left*). Featureplot of human postnatal pituitary displaying expression of *KLF5* (see color scale). Cortico, corticotropes; EC, endothelial cells; IC, immune cells; Lacto, lactotropes; Gonado, gonadotropes; (IL) SC, (intermediate lobe) stem cells (encircled); Somato, somatotropes; Thyro, thyrotropes.

(C) Dotplot displaying average expression (color intensity, see scale) of upregulated immune- and inflammatory response-associated DEGs and proportion of cells (dot size) expressing the specified gene in human pituitary across ages (dataset from[36]). See also Figure S4 and Table S8.

(Figures S4A and S4B). Of note, expression of several of the stem cell markers in the MC (in both human and mouse) may be due to the (partial) overlap of MC (containing FS cells) with the ($SOX2^+$) stem cells, as observed in rat pituitary FS cells.[45] DEG analysis between the stem cells and other cell clusters within each separate dataset revealed still other stem cell markers common to human and mouse pituitary, including WNT- and FGF-related genes (transcription factor 7 like 1 [*TCF7L1*], leucine-rich repeat containing G protein-coupled receptor 4 [*LGR4*]) and *FGFR2* (Figures 4A, 4B, S4C, and Table S8A), in line with the enriched pathways in stem cells as described earlier (Figure 3A). In addition, eyes-absent homolog 4 (*EYA4*) and nuclear factor I B (*NFIB*), transcriptional regulators involved in organogenesis,[51,52] are upregulated in stem cells of both mouse and human pituitaries (Figures 4A, 4B, and S4C).

Finally, we explored whether the increasing inflammatory phenotype of the pituitary stem cells at aging as found in the mouse (see Figures 1D and 1E) is also present in humans using the human postnatal dataset (pediatric, i.e., 2 and 8 years old; adult, i.e., 37 and 41 years old; aged, i.e., 85 and 90 years old).[36] DEG analysis showed in the aged human pituitary stem cells increased expression of genes related to inflammatory response (e.g., annexin A1 [*ANXA1*], *LIFR*, pleiotrophin [*PTN*], selenoprotein S [*SELENOS*], thioredoxin-interacting protein [*TXNIP*]) and to positive regulation of immune response (e.g., signal transducer and activator of transcription 1 [*STAT1*], phospholipase C gamma 2 [*PLCG2*], *B2M*, ribosomal protein L30 [*RPL30*]) (Figure 4C; Table S8B), similar to their enrichment in the mouse stem cell compartment at aging (Figure S4D).

Taken together, the mouse pituitary sc atlas across ages can be interrogated in available human datasets of multiple ages,[36,37] allowing to identify shared molecular patterns, regulatory networks and deduced functions. This cross-species knowledge transfer will accelerate insights in (stem-cell) regulatory

pathways within the human pituitary gland, at present only poorly developed.

DISCUSSION

The pituitary gland plays a pivotal role in the endocrine system, housing a diverse array of cell types responsible for the body's hormonal balances. In this study, we pictured the sc landscape of the male mouse endocrine pituitary by constructing a sc transcriptome atlas of both healthy and perturbed AL across important postnatal ages. As proof of its strong potential, the atlas was applied to explore the puzzling pituitary stem cell population, including phenotypic traits and regulatory mechanisms.

Transcriptomic analysis unveiled a pronounced specificity of the transcription factor KLF5 and the transcription factor complex AP-1 in the stem cells, along with their respective target genes. KLF5 has been reported as positive regulator of stemness in mammary stem cells[53] as well as regulator of stem cell renewal in intestinal stem cells.[46] Deletion of KLF5 in the latter cells resulted in inactivation of NOTCH- and WNT-responsive gene transcription.[46] Given that pituitary stem cells exhibit strong activity of NOTCH and WNT pathways ([9–11] and supported here), KLF5 may play similar roles here in NOTCH/WNT signaling which may explain diminished pituitary organoid growth upon KLF5 inhibition. Analysis of human pituitary sc transcriptomes[36] also revealed enriched expression of *KLF5* in the stem cells, thus advancing KLF5 as a species-conserved pituitary stem cell marker and regulator. Expression of AP-1 subunits, including *Jun*, *Fosl1*, and *Atf* family, was found enriched in the mouse pituitary stem cell compartment, in line with previous work reporting expression of *Jun* in SOX2$^+$ pituitary stem cells by bulk RNA-seq analysis,[11] and JUN colocalization with SOX2$^+$ stem cells in mouse pituitary.[36] Using our pituitary organoid model,[34] we further demonstrated the importance of AP-1 in (SOX2$^+$) stem cells, as inhibition led to abolishment of organoid outgrowth. In human pituitary, the subunits of AP-1 complex were not exclusively expressed in stem cells (see Figures S4A and S4B). On the other hand, we found stem cell markers common in both mouse and human pituitary, including WNT pathway-related genes again (*TCF7L1*, *LGR4*). Together, our sc map and organoid analyses advance the involvement of KLF5 and AP-1 in pituitary stem cell regulation.

Strong indications for the involvement of the EGFR pathway in the stem cell-regulatory niche were found. Multiple pituitary cell types express ligands of the EGF family, whereas stem cells express the cognate receptors. Absence of EGF family ligands abolished organoid growth capacity, while addition of NRG1 and (HB)EGF (as also reported before[34]) activated organoid growth. Within the stem cell compartment, *Nrg1* is most prominently expressed in the proliferating stem cells, and may thus exert an auto-/paracrine function toward stem cell proliferation. HGF is advanced as another regulatory niche factor, being expressed by MC and corticotropes while its receptor *(Met)* is expressed by stem cells, and showing a positive effect on organoid development and growth. These findings align with a recent study describing enhanced *Met* expression[17] in the pituitary stem cells following adrenalectomy, the latter resulting in increased corticotrope number, and a stimulatory effect of HGF on pituisphere formation, a basic readout of pituitary stem cell activity.[4] Also other tissue organoids (e.g., from gastric stem cells) are growth-stimulated when exposed to HGF, similar to EGF stimulation.[54] Lastly, we show that factors from stem cells also affect other cell types, thereby supporting the recent concept that stem cells act as regulatory signaling hub for other cell types in the gland, as has been shown for stem cell-secreted WNT ligands to WNT-responsive committed progenitor cells in neonatal mouse pituitary.[11] In that sense, pituitary stem cells may be peculiar since typical mammalian organ stem cells mainly serve as source of new mature cells during tissue turnover and repair. *Mdk* was found expressed mainly in stem cells and MC and its receptor *Ptprz1* in corticotropes. Exposing mouse corticotrope AtT-20 cells to MDK reduced the expression of the mature corticotrope marker *Pomc*. Hence, stem cells may signal to corticotropes through MDK to retain a precursor state, or reverse the mature corticotrope cells into this stage. This process may be required under certain (patho)physiological conditions in which higher numbers of corticotropes are needed, as for instance after adrenalectomy where pituitary progenitors are needed to contribute through proliferation (followed by differentiation).[1,17] Alternatively, stem cells may directly (down)regulate ACTH production by corticotropes through the inhibitory effect of MDK on *Pomc* expression. Taken together, our newly built pituitary sc atlas enables to decode potential interactions between pituitary stem cells and other local cell types, thereby disentangling the stem cell niche, and in the same manner also between non-stem cell types among each other.

Pituitary stem cell (patho)biology in aging and other challenging conditions such as tissue damage remains elusive. Following damage, multiple genes associated with inflammatory/immune response were found increased in the stem cells, particularly at young-adult age, thereby expanding previous findings.[14] Intriguingly, these genes were already considerably expressed in normal (unperturbed) pituitary stem cells in old mice (in line with results before in middle-aged mice[14]), likely explaining the absence of stem cell activation reaction to damage and of the ensuing regeneration at aging (already from middle-age).[14,16] This rising inflammatory/immune phenotype (inflammaging) is indeed present early at aging (middle-age; as shown before[14] and here) and still further enhances at old age (as shown here). Interestingly, we also found an increasing expression of inflammatory/immune markers in old human pituitary as compared to younger individuals (using the postnatal human pituitary datasets[36]). Moreover, a higher number of immune cells, predominantly monocytes, is present in the aged mouse pituitary, potentially recruited by antigens presented by stem cells (and maybe by other cell types as well). In future studies, our atlas can serve as valuable resource to investigate potential interactions between the immune and stem cells across ages through cell-cell interaction analysis (e.g., using CellPhoneDB). Increased antigen processing in stem cells and more immune cell (activated T cell) infiltration were also noted in aged intestine, findings that supported the participation of stem cells in inflammaging.[39] An elevated immune milieu is known to contribute to inflammaging.[39] Thus, our atlas enables the investigation of altered immune processes in the pituitary gland at aging.

In conclusion, we established a mouse endocrine-pituitary sc transcriptomic atlas which provides a powerful tool to decipher pituitary cell biology across postnatal life, both in healthy and diseased (injured) conditions. In particular, it already showed highly valuable to delve into the still enigmatic stem cell population. We additionally provide a publicly available and easily workable format enabling to localize genes of interest in the atlas (as a loom format using SCope[38]) as well as Seurat objects to analyze gene expression per age and healthy/injured condition. Moreover, our provided atlas will allow to incorporate existing as well as upcoming pituitary sc data focusing on other conditions such as other species or genetically perturbed pituitary, thereby enabling to generate further interesting insights. Moreover, incorporating sc datasets from the female sex will provide insights into sex-specific cellular and transcriptomic peculiarities, as previously demonstrated in adult mice,[25] but not yet performed for other postnatal ages. Finally, the extracted molecular stem-cell findings can be validated using the pituitary organoid model, and translation to humans interrogated using human pituitary datasets. A thorough understanding of the pituitary (stem) cells is not only essential to fully grasp the biology of this central endocrine organ, but also to get insight into burdening pituitary diseases.

Limitations of the study

Our study provides a newly composed sc atlas of the mouse endocrine pituitary across important postnatal ages in both healthy and perturbed (injured) condition. To show its strong potential and usefulness, we applied the atlas to delve into pituitary stem cell complexity and regulation. Evidently, further studies can broaden this still narrow scope to all other pituitary cell types, as well as to more mechanistic investigation (e.g., using genetically modified mouse models, gene editing) to expand the current stem cell-focused functional validation using organoids. Moreover, the number of samples (and cell number per sample) still has to be expanded but the current atlas already provides the asset that new samples can be integrated, thereby taking care of challenges including experimental and batch variability and metadata consistency, as actually required for all contemporary sc atlassing endeavors. In addition, expanding the pituitary atlas to include the female sex (currently only one female sample, i.e., from damaged neonatal pituitary) will be highly valuable given the pituitary's role in sex-specific hormone production and processes. Eventually, such gradually expanding pituitary atlas will enable deep understanding of pituitary cell (patho)biology and function in health and disease across ages.

RESOURCE AVAILABILITY

Lead contact

Further information and requests for resources and reagents should be directed to and will be fulfilled by the lead contact, Hugo Vankelecom (hugo.vankelecom@kuleuven.be).

Materials availability

This study did not generate new unique reagents.

Data and code availability

- All data are available in the main text or the supplementary materials. The raw scRNA-seq data acquired in this study have been deposited in BioStudies ArrayExpress (Database: E-MTAB-14008, database: E-MTAB-14067). Loom files for interactive exploration of the pituitary atlas (all ages; (un)damaged condition) and organoid dataset (all ages) are available via Mendeley Data (https://doi.org/10.17632/bmw74jhfcz.1). Moreover, to facilitate a detailed comparison between various ages and states of damage, the datasets are accessible as annotated Seurat objects on Mendeley Data (https://doi.org/10.17632/bmw74jhfcz.1). Publicly available datasets that were analyzed in this study include: database: E− MTAB- 11337 (BioStudies ArrayExpress, https://www.ebi.ac.uk/biostudies/arrayexpress/studies/E-MTAB-11337), database: E-MTAB-10021 (BioStudies ArrayExpress, https://www.ebi.ac.uk/biostudies/arrayexpress/studies/E-MTAB-10021), GSE142653 (GEO, https://www.ncbi.nlm.nih.gov/geo/query/acc.cgi?acc=GSE142653) and GSE178454 (GEO, https://www.ncbi.nlm.nih.gov/geo/query/acc.cgi?acc=GSE178454).
- This paper does not report original code.
- Any additional information required to reanalyze the data reported in this paper is available from the lead contact upon request.

ACKNOWLEDGMENTS

We thank Thomas Van Brussel, Rogier Schepers, Gino Philips, and Bram Boeckx (D.L.'s group, KU Leuven) for technical and bioinformatical support in the scRNA-seq experiments and the Genomics Core (KU Leuven), especially Álvaro Cortés Calabuig, for running the CellRanger pipeline. The "Vlaams Supercomputer Centrum", overseen by the Fund for Scientific Research Flanders (FWO), supplied the computational resources utilized for scRNA-seq bioinformatic analyses. The funders had no role in study design, data collection and interpretation, or the decision to submit the work for publication. Certain figures were created using BioRender.com. This work was supported by grants from the KU Leuven Research Fund (C14/16/079; KA/20/087) and from the FWO (G0E1417N; G064723N). E.L. (11A3320N), S.D.V. (1S00823N) and B.A (11P8X24N) are supported by a PhD Fellowship from the FWO. F.H. was supported by an FWO project grant (G061819FWO).

AUTHOR CONTRIBUTIONS

Conceptualization: S.D.V., E.L., and H.V.; methodology: S.D.V., E.L., and F.H.; investigation: S.D.V., E.L., B.A., J.H., F.H., and H.V.; resources: D.L. and H.V.; writing: S.D.V., E.L., and H.V.; supervision: H.V.

DECLARATION OF INTERESTS

The authors declare no competing interests.

STAR★METHODS

Detailed methods are provided in the online version of this paper and include the following:

- KEY RESOURCES TABLE
- EXPERIMENTAL MODEL AND STUDY PARTICIPANT DETAILS
  - Mice and *in vivo* treatments
  - Pituitary organoid culture
  - AtT-20 culture and treatment
- METHOD DETAILS
  - Immunostaining analysis
  - Gene expression analysis
  - Single-cell RNA-sequencing analysis
  - Integration of the pituitary single-cell transcriptomes across the targeted ages
  - Integration of the pituitary organoid single-cell transcriptomes and projection on the pituitary single-cell map
  - Differential gene expression and gene ontology analysis
  - Gene-regulatory network and cell-cell communication analyses
  - Atlas gene-expression visualization tool in SCope
  - Human pituitary transcriptomic datasets
- QUANTIFICATION AND STATISTICAL ANALYSIS

SUPPLEMENTAL INFORMATION

Supplemental information can be found online at https://doi.org/10.1016/j.isci.2024.111708.

Received: February 16, 2024
Revised: May 17, 2024
Accepted: December 27, 2024
Published: January 6, 2025

REFERENCES

1. Rizzoti, K., Akiyama, H., and Lovell-Badge, R. (2013). Mobilized adult pituitary stem cells contribute to endocrine regeneration in response to physiological demand. Cell Stem Cell *13*, 419–432. https://doi.org/10.1016/J.STEM.2013.07.006.
2. Andoniadou, C.L., Matsushima, D., Mousavy Gharavy, S.N., Signore, M., Mackintosh, A.I., Schaeffer, M., Gaston-Massuet, C., Mollard, P., Jacques, T.S., Le Tissier, P., et al. (2013). SOX2+ stem/progenitor cells in the adult mouse pituitary support organ homeostasis and have tumor-inducing potential. Cell Stem Cell *13*, 433–445. https://doi.org/10.1016/J.STEM.2013.07.004.
3. Melmed, S. (2005). In The pituitary, 2nd ed., S. Melmed, ed. (Blackwell).
4. Chen, J., Hersmus, N., Van Duppen, V., Caesens, P., Denef, C., and Vankelecom, H. (2005). The adult pituitary contains a cell population displaying stem/progenitor cell and early embryonic characteristics. Endocrinology *146*, 3985–3998. https://doi.org/10.1210/EN.2005-0185.
5. Vankelecom, H., and Chen, J. (2014). Pituitary stem cells: Where do we stand? Mol. Cell. Endocrinol. *385*, 2–17. https://doi.org/10.1016/J.MCE.2013.08.018.
6. Pérez Millán, M.I., Cheung, L.Y.M., Mercogliano, F., Camilletti, M.A., Chirino Felker, G.T., Moro, L.N., Miriuka, S., Brinkmeier, M.L., and Camper, S.A. (2023). Pituitary stem cells: past, present and future perspectives. Nat. Rev. Endocrinol. *20*, 77–92. https://doi.org/10.1038/s41574-023-00922-4.
7. Fauquier, T., Rizzoti, K., Dattani, M., Lovell-Badge, R., and Robinson, I.C.A.F. (2008). SOX2-expressing progenitor cells generate all of the major cell types in the adult mouse pituitary gland. Proc. Natl. Acad. Sci. USA *105*, 2907–2912. https://doi.org/10.1073/PNAS.0707886105.
8. Chen, J., Gremeaux, L., Fu, Q., Liekens, D., Van Laere, S., and Vankelecom, H. (2009). Pituitary progenitor cells tracked down by side population dissection. Stem Cell. *27*, 1182–1195. https://doi.org/10.1002/STEM.51.
9. Laporte, E., Vennekens, A., and Vankelecom, H. (2020). Pituitary remodeling throughout life: Are resident stem cells involved? Front. Endocrinol. *11*, 604519. https://doi.org/10.3389/FENDO.2020.604519.
10. Laporte, E., Hermans, F., De Vriendt, S., Vennekens, A., Lambrechts, D., Nys, C., Cox, B., and Vankelecom, H. (2022). Decoding the activated stem cell phenotype of the neonatally maturing pituitary. Elife *11*, e75742. https://doi.org/10.7554/ELIFE.75742.
11. Russell, J.P., Lim, X., Santambrogio, A., Yianni, V., Kemkem, Y., Wang, B., Fish, M., Haston, S., Grabek, A., Hallang, S., et al. (2021). Pituitary stem cells produce paracrine WNT signals to control the expansion of their descendant progenitor cells. Elife *10*, e59142. https://doi.org/10.7554/ELIFE.59142.
12. Gremeaux, L., Fu, Q., Chen, J., and Vankelecom, H. (2012). Activated phenotype of the pituitary stem/progenitor cell compartment during the early-postnatal maturation phase of the gland. Stem Cell. Dev. *21*, 801–813. https://doi.org/10.1089/SCD.2011.0496.
13. Zhu, X., Tollkuhn, J., Taylor, H., and Rosenfeld, M.G. (2015). Notch-dependent pituitary SOX2+ stem cells exhibit a timed functional extinction in regulation of the postnatal gland. Stem Cell Rep. *5*, 1196–1209. https://doi.org/10.1016/J.STEMCR.2015.11.001.
14. Vennekens, A., Laporte, E., Hermans, F., Cox, B., Modave, E., Janiszewski, A., Nys, C., Kobayashi, H., Malengier-Devlies, B., Chappell, J., et al. (2021). Interleukin-6 is an activator of pituitary stem cells upon local damage, a competence quenched in the aging gland. Proc. Natl. Acad. Sci. USA *118*, e2100052118. https://doi.org/10.1073/PNAS.2100052118.
15. Fu, Q., Gremeaux, L., Luque, R.M., Liekens, D., Chen, J., Buch, T., Waisman, A., Kineman, R., and Vankelecom, H. (2012). The adult pituitary shows stem/progenitor cell activation in response to injury and is capable of regeneration. Endocrinology *153*, 3224–3235. https://doi.org/10.1210/EN.2012-1152.
16. Willems, C., Fu, Q., Roose, H., Mertens, F., Cox, B., Chen, J., and Vankelecom, H. (2016). Regeneration in the pituitary after cell-ablation injury: Time-related aspects and molecular analysis. Endocrinology *157*, 705–721. https://doi.org/10.1210/EN.2015-1741.
17. Rizzoti, K., Chakravarty, P., Sheridan, D., and Lovell-Badge, R. (2023). SOX9-positive pituitary stem cells differ according to their position in the gland and maintenance of their progeny depends on context. Sci. Adv. *9*, eadf6911. https://doi.org/10.1126/SCIADV.ADF6911.
18. Nys, C., Lee, Y.L., Roose, H., Mertens, F., De Pauw, E., Kobayashi, H., Sciot, R., Bex, M., Versyck, G., De Vleeschouwer, S., et al. (2022). Exploring stem cell biology in pituitary tumors and derived organoids. Endocr. Relat. Cancer *29*, 427–450. https://doi.org/10.1530/ERC-21-0374.
19. Mertens, F., Gremeaux, L., Chen, J., Fu, Q., Willems, C., Roose, H., Govaere, O., Roskams, T., Cristina, C., Becú-Villalobos, D., et al. (2015). Pituitary tumors contain a side population with tumor stem cell-associated characteristics. Endocr. Relat. Cancer *22*, 481–504. https://doi.org/10.1530/ERC-14-0546.
20. Franceschi, C., and Campisi, J. (2014). Chronic inflammation (inflammaging) and its potential contribution to age-associated diseases. J. Gerontol. A Biol. Sci. Med. Sci. *69*, S4–S9. https://doi.org/10.1093/GERONA/GLU057.
21. Cheung, L.Y.M., George, A.S., McGee, S.R., Daly, A.Z., Brinkmeier, M.L., Ellsworth, B.S., and Camper, S.A. (2018). Single-cell RNA sequencing reveals novel markers of male pituitary stem cells and hormone-producing cell types. Endocrinology *159*, 3910–3924. https://doi.org/10.1210/EN.2018-00750.
22. Mayran, A., Sochodolsky, K., Khetchoumian, K., Harris, J., Gauthier, Y., Bemmo, A., Balsalobre, A., and Drouin, J. (2019). Pioneer and nonpioneer factor cooperation drives lineage specific chromatin opening. Nat. Commun. *10*, 3807–3813. https://doi.org/10.1038/s41467-019-11791-9.
23. Miles, T.K., Odle, A.K., Byrum, S.D., Lagasse, A., Haney, A., Ortega, V.G., Bolen, C.R., Banik, J., Reddick, M.M., Herdman, A., et al. (2023). Anterior pituitary transcriptomics following a high-fat diet: Impact of oxidative stress on cell metabolism. Endocrinology *165*, bqad191. https://doi.org/10.1210/ENDOCR/BQAD191.
24. Yan, T., Wang, R., Yao, J., and Luo, M. (2023). Single-cell transcriptomic analysis reveals rich pituitary–immune interactions under systemic inflammation. PLoS Biol. *21*, e3002403. https://doi.org/10.1371/JOURNAL.PBIO.3002403.
25. Ruf-Zamojski, F., Zhang, Z., Zamojski, M., Smith, G.R., Mendelev, N., Liu, H., Nudelman, G., Moriwaki, M., Pincas, H., Castanon, R.G., et al. (2021). Single nucleus multi-omics regulatory landscape of the murine pituitary. Nat. Commun. *12*, 2677. https://doi.org/10.1038/s41467-021-22859-w.
26. Ruggiero-Ruff, R.E., Le, B.H., Villa, P.A., Lainez, N.M., Athul, S.W., Das, P., Ellsworth, B.S., and Coss, D. (2024). Single-cell transcriptomics identifies pituitary gland changes in diet-induced obesity in male mice. Endocrinology *165*, bqad196. https://doi.org/10.1210/ENDOCR/BQAD196.
27. Cheung, L.Y.M., and Camper, S.A. (2020). PROP1-dependent retinoic acid signaling regulates developmental pituitary morphogenesis and hormone expression. Endocrinology *161*, bqaa002. https://doi.org/10.1210/ENDOCR/BQAA002.
28. Ho, Y., Hu, P., Peel, M.T., Chen, S., Camara, P.G., Epstein, D.J., Wu, H., and Liebhaber, S.A. (2020). Single-cell transcriptomic analysis of adult mouse pituitary reveals sexual dimorphism and physiologic demand-induced cellular plasticity. Protein Cell *11*, 565–583. https://doi.org/10.1007/s13238-020-00705-x.

29. García Solá, M.E., Stedile, M., Beckerman, I., and Kordon, E.C. (2021). An integrative single-cell transcriptomic atlas of the post-natal mouse mammary gland allows discovery of new developmental trajectories in the luminal compartment. J. Mammary Gland Biol. Neoplasia *26*, 29–42. https://doi.org/10.1007/s10911-021-09488-1.

30. Lake, B.B., Menon, R., Winfree, S., Hu, Q., Melo Ferreira, R., Kalhor, K., Barwinska, D., Otto, E.A., Ferkowicz, M., Diep, D., et al. (2023). An atlas of healthy and injured cell states and niches in the human kidney. Nature *619*, 585–594. https://doi.org/10.1038/s41586-023-05769-3.

31. Hermans, F., Bueds, C., Hemeryck, L., Lambrichts, I., Bronckaers, A., and Vankelecom, H. (2022). Establishment of inclusive single-cell transcriptome atlases from mouse and human tooth as powerful resource for dental research. Front. Cell Dev. Biol. *10*, 1021459–1021519. https://doi.org/10.3389/FCELL.2022.1021459.

32. Marečková, M., Garcia-Alonso, L., Moullet, M., Lorenzi, V., Petryszak, R., Sancho-Serra, C., Oszlanczi, A., Icoresi Mazzeo, C., Wong, F.C.K., Kelava, I., et al. (2024). An integrated single-cell reference atlas of the human endometrium. Nat. Genet. *56*, 1925–1937. https://doi.org/10.1038/s41588-024-01873-w.

33. Laporte, E., and Vankelecom, H. (2023). Organoid models of the pituitary gland in health and disease. Front. Endocrinol. *14*, 1233714–1233812. https://doi.org/10.3389/FENDO.2023.1233714.

34. Cox, B., Laporte, E., Vennekens, A., Kobayashi, H., Nys, C., Van Zundert, I., Ujii, H., Vercauteren Drubbel, A., Beck, B., Roose, H., et al. (2019). Organoids from pituitary as a novel research model toward pituitary stem cell exploration. J. Endocrinol. *240*, 287–308. https://doi.org/10.1530/JOE-18-0462.

35. Laporte, E., Nys, C., and Vankelecom, H. (2022). Development of organoids from mouse pituitary as in vitro model to explore pituitary stem cell biology. J. Vis. Exp. *180*, e63431. https://doi.org/10.3791/63431.

36. Zhang, Z., Zamojski, M., Mendelev, N., Willis, T.L., Zamojski, M., Yianni, V., Pincas, H., Seenarine, N., Amper, M.A.S., Vasoya, M., et al. (2022). Single nucleus transcriptome and chromatin accessibility of postmortem human pituitaries reveal diverse stem cell regulatory mechanisms. Cell Rep. *38*, 110467–110517. https://doi.org/10.1016/J.CELREP.2022.110467.

37. Zhang, S., Cui, Y., Ma, X., Yong, J., Yan, L., Yang, M., Ren, J., Tang, F., Wen, L., and Qiao, J. (2020). Single-cell transcriptomics identifies divergent developmental lineage trajectories during human pituitary development. Nat. Commun. *11*, 5275–5316. https://doi.org/10.1038/s41467-020-19012-4.

38. Davie, K., Janssens, J., Koldere, D., De Waegeneer, M., Pech, U., Kreft, Ł., Aibar, S., Makhzami, S., Christiaens, V., Bravo González-Blas, C., et al. (2018). A single-cell transcriptome atlas of the aging drosophila brain. Cell *174*, 982–998.e20. https://doi.org/10.1016/J.CELL.2018.05.057.

39. Funk, M.C., Gleixner, J.G., Heigwer, F., Vonficht, D., Valentini, E., Aydin, Z., Tonin, E., Del Prete, S., Mahara, S., Throm, Y., et al. (2023). Aged intestinal stem cells propagate cell-intrinsic sources of inflammaging in mice. Dev. Cell *58*, 2914–2929.e7. https://doi.org/10.1016/j.devcel.2023.11.013.

40. Ponnappan, S., and Ponnappan, U. (2011). Aging and immune function: Molecular mechanisms to interventions. Antioxidants Redox Signal. *14*, 1551–1585. https://doi.org/10.1089/ars.2010.3228.

41. Li, X., Li, C., Zhang, W., Wang, Y., Qian, P., and Huang, H. (2023). Inflammation and aging : signaling pathways and intervention therapies. Signal Transduct. Targeted Ther. *8*, 239–329. https://doi.org/10.1038/s41392-023-01502-8.

42. Janky, R., Verfaillie, A., Imrichová, H., Van de Sande, B., Standaert, L., Christiaens, V., Hulselmans, G., Herten, K., Naval Sanchez, M., Potier, D., et al. (2014). iRegulon: From a gene list to a gene regulatory network using large motif and track collections. PLoS Comput. Biol. *10*, e1003731. https://doi.org/10.1371/journal.pcbi.1003731.

43. Shin, J., Berg, D.A., Zhu, Y., Shin, J.Y., Song, J., Bonaguidi, M.A., Enikolopov, G., Nauen, D.W., Christian, K.M., Ming, G.-L., and Song, H. (2015). Single-cell RNA-seq with waterfall reveals molecular cascades underlying adult neurogenesis. Cell Stem Cell *17*, 360–372. https://doi.org/10.1016/J.STEM.2015.07.013.

44. Fujiwara, K., Tsukada, T., Horiguchi, K., Fujiwara, Y., Takemoto, K., Nio-Kobayashi, J., Ohno, N., and Inoue, K. (2020). Aldolase C is a novel molecular marker for folliculo-stellate cells in rodent pituitary. Cell Tissue Res. *381*, 273–284. https://doi.org/10.1007/s00441-020-03200-1.

45. Fletcher, P.A., Smiljanic, K., Prévide, R.M., Constantin, S., Sherman, A.S., Coon, S.L., and Stojilkovic, S.S. (2023). The astroglial and stem cell functions of adult rat folliculostellate cells. Glia *71*, 205–228. https://doi.org/10.1002/GLIA.24267.

46. Kim, C.K., Saxena, M., Maharjan, K., Song, J.J., Shroyer, K.R., Bialkowska, A.B., Shivdasani, R.A., and Yang, V.W. (2020). Krüppel-like Factor 5 regulates stemness, lineage specification, and regeneration of intestinal epithelial stem cells. Cell. Mol. Gastroenterol. Hepatol. *9*, 587–609. https://doi.org/10.1016/J.JCMGH.2019.11.009.

47. Kinisu, M., Choi, Y.J., Cattoglio, C., Liu, K., Roux de Bezieux, H., Valbuena, R., Pum, N., Dudoit, S., Huang, H., Xuan, Z., et al. (2021). Klf5 establishes bi-potential cell fate by dual regulation of ICM and TE specification genes. Cell Rep. *37*, 109982–110014. https://doi.org/10.1016/J.CELREP.2021.109982.

48. Aibar, S., González-Blas, C.B., Moerman, T., Huynh-Thu, V.A., Imrichova, H., Hulselmans, G., Rambow, F., Marine, J.C., Geurts, P., Aerts, J., et al. (2017). SCENIC: single-cell regulatory network inference and clustering. Nat. Methods *14*, 1083–1086. https://doi.org/10.1038/NMET.4463.

49. Garcia-Alonso, L., Lorenzi, V., Mazzeo, C.I., Alves-Lopes, J.P., Roberts, K., Sancho-Serra, C., Engelbert, J., Marečková, M., Gruhn, W.H., Botting, R.A., et al. (2022). Single-cell roadmap of human gonadal development. Nature *607*, 540–547. https://doi.org/10.1038/s41586-022-04918-4.

50. Uchikawa, E., Chen, Z., Xiao, G.-Y., Zhang, X., and Bai, X.C. (2021). Structural basis of the activation of c-MET receptor. Nat. Commun. *12*, 4074. https://doi.org/10.1038/s41467-021-24367-3.

51. Rayapureddi, J.P., Kattamuri, C., Steinmetz, B.D., Frankfort, B.J., Ostrin, E.J., Mardon, G., and Hegde, R.S. (2003). Eyes absent represents a class of protein tyrosin phosphatases. Nature *426*, 295–298.

52. Steele-Perkins, G., Plachez, C., Butz, K.G., Yang, G., Bachurski, C.J., Kinsman, S.L., Litwack, E.D., Richards, L.J., and Gronostajski, R.M. (2005). The transcription factor gene Nfib is essential for both lung maturation and brain development. Mol. Cell Biol. *25*, 685–698. https://doi.org/10.1128/MCB.25.2.685-698.2005.

53. Liu, R., Shi, P., Zhou, Z., Zhang, H., Li, W., Zhang, H., and Chen, C. (2018). Krüpple-like factor 5 is essential for mammary gland development and tumorigenesis. J. Pathol. *246*, 497–507. https://doi.org/10.1002/PATH.5153.

54. Jangphattananont, N., Sato, H., Imamura, R., Sakai, K., Terakado, Y., Murakami, K., Barker, N., Oshima, H., Oshima, M., Takagi, J., et al. (2019). Distinct localization of mature HGF from its precursor form in developing and repairing the stomach. Int. J. Mol. Sci. *20*, 2955. https://doi.org/10.3390/IJMS20122955.

55. Luque, R.M., Amargo, G., Ishii, S., Lobe, C., Franks, R., Kiyokawa, H., and Kineman, R.D. (2007). Reporter expression, induced by a growth hormone promoter-driven Cre recombinase (rGHp-Cre) transgene, questions the developmental relationship between somatotropes and lactotropes in the adult mouse pituitary gland. Endocrinology *148*, 1946–1953. https://doi.org/10.1210/en.2006-1542.

56. Buch, T., Heppner, F.L., Tertilt, C., Heinen, T.J.A.J., Kremer, M., Wunderlich, F.T., Jung, S., and Waisman, A. (2005). A Cre-inducible diphtheria toxin receptor mediates cell lineage ablation after toxin administration. Nat. Methods *2*, 419–426. https://doi.org/10.1038/nmeth762.

57. Schindelin, J., Arganda-Carreras, I., Frise, E., Kaynig, V., Longair, M., Pietzsch, T., Preibisch, S., Rueden, C., Saalfeld, S., Schmid, B., et al. (2012). Fiji: an open-source platform for biological-image analysis. Nat. Methods *9*, 676–682. https://doi.org/10.1038/nmeth.2019.

58. McDavid, A. & Finak, G. Y. M. (2023). MAST: Model-based analysis of single cell transcriptomics. 10.18129/B9.bioc.MAST.

59. Young, M.D., and Behjati, S. (2020). SoupX removes ambient RNA contamination from droplet-based single-cell RNA sequencing data. GigaScience *9*, giaa151. https://doi.org/10.1093/GIGASCIENCE/GIAA151.

60. Thomas, P.D., Ebert, D., Muruganujan, A., Mushayahama, T., Albou, L.P., and Mi, H. (2022). PANTHER: Making genome-scale phylogenetics accessible to all. Protein Sci. *31*, 8–22. https://doi.org/10.1002/PRO.4218.

61. Efremova, M., Vento-Tormo, M., Teichmann, S.A., and Vento-Tormo, R. (2020). CellPhoneDB: inferring cell–cell communication from combined expression of multi-subunit ligand–receptor complexes. Nat. Protoc. *15*, 1484–1506. https://doi.org/10.1038/s41596-020-0292-x.

62. Stuart, T., Butler, A., Hoffman, P., Hafemeister, C., Papalexi, E., Mauck, W.M., 3rd, Hao, Y., Stoeckius, M., Smibert, P., and Satija, R. (2019). Comprehensive integration of single-cell data resource comprehensive integration of single-cell data. Cell *177*, 1888–1902.e21. https://doi.org/10.1016/J.CELL.2019.05.031.

63. Hao, Y., Hao, S., Andersen-Nissen, E., Mauck, W.M., Zheng, S., Butler, A., Lee, M.J., Wilk, A.J., Darby, C., Zager, M., et al. (2021). Integrated analysis of multimodal single-cell data. Cell *184*, 3573–3587.e29. https://doi.org/10.1016/J.CELL.2021.04.048.

64. Suo, S., Zhu, Q., Saadatpour, A., Fei, L., Guo, G., and Yuan, G.C. (2018). Revealing the critical regulators of cell identity in the mouse cell atlas. Cell Rep. *25*, 1436–1445.e3. https://doi.org/10.1016/J.CELREP.2018.10.045.

STAR★METHODS

KEY RESOURCES TABLE

REAGENT or RESOURCE	SOURCE	IDENTIFIER
Antibodies		
Mouse monoclonal anti-ACTH	Thermo Fisher Scientific	CAT#5443-MSM2-P0
Rabbit polyclonal anti-ALDOC	Thermo Fisher Scientific	CAT#PA5-27659; RRID: AB_2545135
Rabbit polyclonal anti-KLF5	Thermo Fisher Scientific	CAT#PA5-27876; RRID: AB_2545352
Rabbit polyclonal anti-PTPRZ1	Thermo Fisher Scientific	CAT#PA5-101832; RRID: AB_2851264
Goat polyclonal anti-SOX2	Immune Systems	CAT#GT15098; RRID: AB_2732043
Donkey polyclonal anti-goat IgG 555	Thermo Fisher Scientific	CAT#A-21432; RRID: AB_2535853
Donkey polyclonal anti-mouse IgG 555	Thermo Fisher Scientific	CAT#A-31570; RRID: AB_2536180
Donkey polyclonal anti-rabbit IgG 488	Thermo Fisher Scientific	CAT#A-21206; RRID: AB_2535792
Chemicals, peptides, and recombinant proteins		
Diphtheria toxin	Merck	CAT#D0564
Matrigel	Corning	CAT#356234
Human Heregulin beta-1 Recombinant Protein	Peprotech	CAT#100-03
Human HGF Recombinant Protein	Peprotech	CAT#100-39
Human Midkine (MK) Recombinant Protein	Peprotech	CAT#450-16
SGX523	Selleckchem	CAT# S1112
CID 5951923	MedChemExpress	CAT#HY-W011044
CL-387785 (EKI-785)	Selleckchem	CAT#S7557
SR 11302	MedChemExpress	CAT#HY-15870
Critical commercial assays		
10× Chromium 3′ v3.1 chemistry library prep	10× Genomics	CAT#1000268
RNeasy Micro kit	Qiagen	CAT#74004
Superscript III First-Strand Synthesis Supermix	Invitrogen	CAT#18080400
SYBR^{TM} Green PCR Master Mix	Thermo Fisher Scientific	CAT#4309155
Deposited data		
Raw scRNA-seq data	This paper; BioStudies ArrayExpress	Database: E-MTAB-14008; Database: E-MTAB-14067
Analyzed scRNA-seq data	This paper; Mendeley Data	https://doi.org/10.17632/bmw74jhfcz.1 and https://doi.org/10.17632/bmw74jhfcz.1
Published scRNA-seq data of mouse pituitary	Laporte et al.[10]; Vennekens et al.[14]; BioStudies ArrayExpress	Database: E-MTAB-11337; Database: E-MTAB- 10021; Database: E-MTAB- 10021
Published scRNA-seq data of human fetal pituitary	Zhang et al.[37]	GSE142653
Published snRNA-seq data of human postnatal pituitary	Zhang et al.[36]	GSE178454
Experimental models: Cell lines		
AtT-20	ATCC	CAT#CCL-89; RRID: CVCL_2300
Experimental models: Organisms/strains		
Mouse: GH$^{Cre/+}$; Tg(Gh1-cre)bKnmn	Luque et al.[55]	MGI:4442901
Mouse: R26$^{iDTR/+}$; Gt(ROSA)26Sor$^{tm1(HBEGF)Awai}$; -/iDTR	Buch et al.[56]	MGI:3772576; RRID:IMSR_JAX:007900
Oligonucleotides		
Primer used in RT-qPCR see Table S9	iDT; this paper	N/A

(*Continued on next page*)

Continued

REAGENT or RESOURCE	SOURCE	IDENTIFIER
Software and algorithms		
GraphPad Prism Software	GraphPad Prism	https://www.graphpad.com/; Version 9.5.1; RRID:SCR_002798
Fiji	Schindelin et al.[57]	https://imagej.net/; RRID:SCR_002285
IncuCyte S3 software	Sartorius	https://www.sartorius.com/en/products/live-cell-imaging-analysis/live-cell-analysis-software/incucyte-s3-software-v2018b
CellRanger	10x Genomics	Version 5.0.0; Version 6.0.2
Seurat	Satija Lab and Collaborators	https://satijalab.org/seurat/; Version 4
MAST	McDavid et al.[58]	N/A
SoupX	Young et al.[59]	Version 1.5.0
BioRender	BioRender	https://www.biorender.com/
PANTHER	Thomas et al.[60]	www.pantherdb.org; Version 19.0
Venn diagram	VIB/UGent	https://bioinformatics.psb.ugent.be/webtools/Venn/
pySCENIC	Aibar et al.[48]	Version 0.9.15
iRegulon application in Cytoscape	Janky et al.[42]	Version 1.3; Version 3.10.1
CellPhoneDB	Efremova et al.[61]	Version 2.1.5
Loompy	Linnarsson Lab	www.loompy.org; Version 2.0.17

EXPERIMENTAL MODEL AND STUDY PARTICIPANT DETAILS

Mice and *in vivo* treatments

C57BL/6J mice were used for the experiments. Mice were housed in Type II cages in conditions of constant temperature (22 ± 2°C), 45–70% humidity and 14-h light, 10-h dark cycle (lights on at 7 a.m.). The animals had *ad libitum* access to chow and water. The mice were housed in groups of up to 5 same-sex littermates. Sex and age of all animals used for scRNA-sequencing and RT-qPCR are provided in Table S1. For all other experiments, young-adult (8–12 weeks) male, middle-aged (12–15 months) and old (24–26 months) male mice were used. All animal experiments were approved by the KU Leuven Ethical Committee for Animal Experimentation (P153/2018 and P165/2023).

To inflict local damage in the pituitary, $Gh^{Cre/+}$ mice (Tg(Gh1-cre)bKnmn[55]) were crossed with $ROSA26^{iDTR/iDTR}$ animals (Gt(ROSA)26Sor$^{tm1(HBEGF)Awai}$; RRID:IMSR_JAX:007900[56]). The resulting $Gh^{Cre/+}$;$ROSA26^{iDTR/+}$ mice and $Gh^{+/+}$;$ROSA26^{iDTR/+}$ control littermates were intraperitoneally injected with diphtheria toxin (DT, 4 ng/g body weight; Merck, Darmstadt, Germany) for 3 consecutive days, leading to somatotrope-cell ablation (all as described before[14–16]). Pituitaries (damaged and control) were isolated and analyzed the day after the 3-day DT injection.

Pituitary organoid culture

Pituitary organoid cultures were established as in detail described before.[34,35] In short, AL cells were seeded in droplets of Matrigel (Corning, New York, NY), cultured in previously defined pituitary organoid medium (PitOM) and incubated at 37°C in 5% CO_2.[10,34] Organoid cultures were expanded and passaged (i.e., reseeding of organoid fragments) every 10–14 days as previously described.[34,35] Experiments were performed using early-passage (i.e., passage (P) 3) pituitary organoids and pituitary (stem cell) identity was assessed by pituitary stem cell marker expression validation. Organoid morphology was constantly monitored during culture and mycoplasma tests were routinely performed, indicating absence of infections. For each organoid experiment, the biological sample size and allocation to experimental groups can be found in the corresponding figure legends.

To explore their effects on organoid formation and growth, NRG1 (200 ng/mL; Peprotech, London, UK), HGF (20 ng/mL, Peprotech), SGX523 (cMET inhibitor, 200 nM, Selleckchem, Houston, TX), SR11302 (AP-1 inhibitor, 100 μM; MedChemExpress, Monmouth Junction, NJ), EKI-785 (EGFR inhibitor, 1 μM; Selleckchem) and CID 5951923 (KLF5 inhibitor, 10 μM; MedChemExpress) were added to the organoid medium for 10 days after AL cell seeding (P0), or vehicle (DMSO) as control.

Brightfield time-lapse images were recorded with the Incucyte S3 (Sartorius, Göttingen, Germany) every 6 h for 10 days using the included Organoid Module. Organoid count and area were analyzed for each time point using the Incucyte Organoid Analysis Software. Organoid count and area for each time point was normalized to the average organoid area recorded at endpoint in the control condition (PitOM).

AtT-20 culture and treatment

The mouse corticotrope AtT-20 cell line was obtained from American Type Culture Collection (ATCC, Manassas, VA; RRID: CVCL_2300). Cells were cultured in Ham's F-12K (Kaighn's) medium (Thermo Fisher Scientific) supplemented with 15% horse serum (Thermo Fisher Scientific) and 2.5% fetal bovine serum (Sigma-Aldrich, St. Louis, MO). Medium was refreshed 2–3 times a week. AtT-20 cells were exposed to MDK (1-10-100 ng/mL; Peprotech) for 7 days. Routine mycoplasma testing was performed showing no infections, and corticotrope identity validated using reverse transcription (RT) quantitative PCR (RT-qPCR) for associated genes (*Pomc*, *Tbx19*). Other cell authentication was not included. The experiment was performed with three biological replicates per treatment.

METHOD DETAILS

Immunostaining analysis

Pituitaries and organoids were fixed in 4% paraformaldehyde (PFA; Merck, Darmstadt, Germany) and embedded in paraffin using the Excelsior ES Tissue Processor and Epredia HistoStar Embedding Workstation (Fisher Scientific, Hampton, NH). Immunofluorescence staining of 5-μm sections was performed as described before.[10,14,34] Antigen retrieval in citrate buffer was followed by permeabilization with Triton X-100 (Merck) and blocking with bovine serum albumin, glycine and donkey serum (Merck). Following incubation with primary and secondary antibodies (key resources table) and nuclear counterstaining with Hoechst33342 (Merck), sections were mounted with ProLong Gold (Thermo Fisher Scientific, Waltham, MA).

Images were recorded using a Leica DM5500 upright epifluorescence microscope (Leica Microsystems, Wetzlar, Germany) accessible through the Imaging Core (VIB, KU Leuven), and converted to pictures for figures with Fiji imaging software (version 2.9.0).[57]

Gene expression analysis

Total RNA from AL cells and derived organoids (at P3) was isolated using the RNeasy Micro kit (Qiagen, Hilden, Germany) and subjected to RT with Superscript III First-Strand Synthesis Supermix (Invitrogen, Waltham, MA). Following RT, qPCR was performed using the Platinum SYBR Green qPCR SuperMix-UDG (Invitrogen) and specific forward and reverse primers (Table S9), as described before.[34] β-actin (*Actb*) was used as housekeeping gene for normalization. Normalized gene expression levels are shown as bar graphs of ΔCt values (Ct target − Ct housekeeping gene).

Single-cell RNA-sequencing analysis

Sc transcriptomic data from neonatal (postnatal day 7), young-adult (8–12 weeks) and middle-aged (12–15 months) AL (male mice, except male and female together at neonatal stage) were acquired before.[10,14] Here, additional scRNA-seq analyses were performed on the AL of old male mice and on pituitary organoids (See Graphical Abstract; Table S1).

The AL of DT-injected elderly $Gh^{Cre/+}$;$ROSA26^{iDTR/+}$ and $Gh^{+/+}$;$ROSA26^{iDTR/+}$ mice (24–26 months old males; $n = 2$ of each) were isolated and dispersed into single cells using trypsin (Thermo Fisher Scientific), all as previously described in detail.[4,8,35] Organoids were established from undamaged AL at all ages, and were expanded until P3. Organoids were then dispersed into single cells using TrypLE Express (Thermo Fisher Scientific) and mechanical dissociation, filtered through a 40 μm filter and subjected to scRNA-seq analyses using 10x Genomics technology (Pleasanton, CA). Cells were loaded onto a cartridge and sc capture, barcoding and library preparation performed using 10x Chromium 3′ v3.1 chemistry according to the manufacturer's protocol (10x Genomics). Libraries were sequenced using a NovaSeq 6000 (Illumina, San Diego, CA).

Next, the raw sequencing reads of all ages (neonatal (E-MTAB-11337),[10] young-adult (E-MTAB-10021),[14] middle-aged (E-MTAB-10021)[14] and old (this study)) in both healthy (undamaged) and damaged condition were demultiplexed and aligned to the mouse reference genome (GRCm39-2024-A), and gene expression matrices were generated, all according to the CellRanger pipeline (v6.0.2; 10x Genomics). The raw sequencing reads of the organoid dataset underwent the same processes. Resultant count matrices of all datasets were further processed in R (v.4.0.2) using Seurat (v4.2.0)[62,63]. Next, doublets and low-quality/dead cells were eliminated based on number of genes and proportion of mitochondrial genes expressed per cell (Table S1), resulting in 93,022 good-quality cells (Table S1). Background/ambient RNA was quantified and removed using SoupX package (v.1.5.0).[59] The global contamination of estimated ambient RNA was well within the common range of 0–10%. The SoupX-filtered expression matrices were then loaded into Seurat.

Integration of the pituitary single-cell transcriptomes across the targeted ages

Next, pituitary scRNA-seq datasets of all ages in both healthy (undamaged) and damaged condition were integrated. Eventually, 67,374 good-quality single cells form the pituitary datasets along the postnatal ages (Table S1). Integration was performed using a Seurat's reference-based approach (with young-adult AL dataset as reference)[62], and data were integrated across all features. The top 30 PCs were selected and used for UMAP dimensionality reduction, resulting in 26 clusters (with clustering resolution set to 0.6 using FindClusters function). Clusters were annotated based on previous publications,[10,14] resulting in 18 cell groups. The AddModuleScore function from Seurat was employed to assess the expression of gene marker profiles, referred to as 'gene modules'. Each cell is assigned a module score determined by the difference between the average expression levels of genes within the module and randomly chosen control features.

Integration of the pituitary organoid single-cell transcriptomes and projection on the pituitary single-cell map

The scRNA-seq datasets of the pituitary organoids from the different ages were integrated as described above and projected onto the pituitary (AL) atlas using Seurat's FindTransferAnchors function (30 dims), TransferData function (30 dims) and MapQuery function, to understand how cells of the query dataset (i.e., organoids) compare to, and align with, the cell clusters of the reference dataset (i.e., AL cell atlas).

Differential gene expression and gene ontology analysis

Differential gene expression analysis was performed using the FindMarkers function with default parameters (with min. pct = 0.25) and using MAST as test method (MAST package; v1.16.0).[58] GO analysis of biological processes and terms was done on the significant DEGs (FDR $\leq$0.05 and avg_log2FC $\geq$ 0.25) using Panther classification system (biological process complete and Reactome pathways; v.19.0).[60] Entire gene lists of these Panther classification systems were retrieved from the website (www.pantherdb.org) and compared to DEGs for some conditions. Common DEGs between conditions were determined and visualized as Venn diagrams using the Bio-informatics & Evolutionary Genomics web application (https://bioinformatics.psb.ugent.be/webtools/Venn/). Of note, the specific stem cell clusters used in DEG/GO analysis as well as other interrogations (i.e., regulon analysis) depended on the specific research question, and are specified in the figures and their legends. For instance, SC1 + SC2 (excluding prolif SC) was used if the stem cell population was analyzed across the ages, since SC1 and SC2 are present at all ages while the prolif SC is virtually only present in neonatal pituitary.

Gene-regulatory network and cell-cell communication analyses

Gene-regulatory networks (regulons) were determined using the SC1 + SC2 clusters of all ages combined in our integrated undamaged pituitary dataset by applying pySCENIC, (v.0.9.15),[48] as described before.[10,14] Co-expression modules were generated, and regulons inferred with default parameters (by using mm10__refseq-r80__10kb_up_and_down_tss.mc9nr and mm10__refseq-r80__500bp_up_and_100 bp_down_tss.mc9nr motif collections). The analysis resulted in a matrix of AUCell values that represent the activity of each regulon in each cell. The cell-type specificity of a regulon (i.e., regulon specificity scores (RSS), calculated using the SCENIC function regulon_specificity_scores[64]) and mean activity of each regulon per cluster (i.e., mean regulon activity (MRA)) were determined. Each score was scaled by min-max normalization. Both scores were visualized as scatterplots, as described before.[31] Extended analysis of the target genes of specific regulons was conducted in Cytoscape (v3.10.1) using the iRegulon application (v1.3).[42]

Ligand-receptor interactions between cell clusters were calculated using the CellPhoneDB package (v2.1.5)[61] based on the normalized count matrices. Prior to running the analysis, mouse gene names were converted to their human orthologues as CellPhoneDB package is based on human gene databases.

Atlas gene-expression visualization tool in SCope

To visualize and interactively explore the newly composed pituitary sc transcriptomic atlas, loom files were established (see data and code availability) that can be uploaded into SCope (available from https://scope.aertslab.org).[38] Separate loom files were made for the pituitary scRNA-seq dataset (all conditions combined) and the pituitary stem cell-derived organoid sc RNA-seq dataset (all ages combined using Loompy v2.0.17 (Linnarsson lab, www.loompy.org).

Human pituitary transcriptomic datasets

Publicly available human fetal pituitary sc (GSE142653)[37] and postnatal pituitary single-nucleus (GSE178454)[36] datasets were retrieved from Gene Expression Omnibus. The human fetal dataset was imported and analyzed as we previously described.[10] SoupX analysis was performed as explained above to remove background/ambient RNA contamination, quantified as 5.1%. The postnatal dataset was individually imported in Seurat for further downstream analyses.[62,63] Following quality control and integration, expression levels were scaled, centered and subjected to PCA. UMAP dimensionality reduction was performed with the top 20 PCs.

QUANTIFICATION AND STATISTICAL ANALYSIS

Statistical analysis was performed using Graphpad Prism (v9.5.1; GraphPad Software, San Diego, CA). (Un-)paired two-tailed Student's t test was applied for comparison of 2 groups. When comparing more groups, one-way analysis of variance (ANOVA) was used when considering one variable, and two-way ANOVA in case of 2 independent variables, followed by the correct multiple comparisons test. Statistical significance was defined as $p < 0.05$. Statistical details of experiments can be found in figure legends.